Journal of Inflammation Research

Dovepress
open access to scientific and medical research

Open Access Full Text Article

ORIGINAL RESEARCH

Magnoflorine Ameliorates Collagen-Induced Arthritis by Suppressing the Inflammation Response via the NF-κB/MAPK Signaling Pathways

Lei Wang[1,*], Pengfei Li[2,*], Yu Zhou[1], Renjun Gu[3], Ge Lu[4], Chunbing Zhang[1,2,5]

[1]College of First Clinical Medicine, Nanjing University of Chinese Medicine, Nanjing, Jiangsu, 210023, People's Republic of China; [2]Department of Clinical Laboratory, Jiangsu Province Hospital of Chinese Medicine, The Affiliated Hospital of Nanjing University of Chinese Medicine, Nanjing, Jiangsu, 210029, People's Republic of China; [3]School of Chinese Medicine & School of Integrated Chinese and Western Medicine, Nanjing University of Chinese Medicine, Nanjing, Jiangsu, 210023, People's Republic of China; [4]College of Acupuncture-Moxibustion and Tuina, Nanjing University of Chinese Medicine, Nanjing, Jiangsu, 210023, People's Republic of China; [5]State Key Laboratory of Ultrasound in Medicine and Engineering, Chongqing Medical University, Chongqing, 400016, People's Republic of China

*These authors contributed equally to this work

Correspondence: Chunbing Zhang, Department of Clinical Laboratory, Jiangsu Province Hospital of Chinese Medicine, Affiliated Hospital of Nanjing University of Chinese Medicine, Nanjing, 210029, People's Republic of China, Email chunbingzhang@njucm.edu.cn

Objective: Magnoflorine (Mag) has been reported to have anxiolytics, anti-cancer, and anti-inflammatory properties. In this study, we aim to investigate the effects of Mag on the rheumatoid arthritis (RA) and explore the underlying mechanism using a collagen-induced arthritis (CIA) mouse model and a lipopolysaccharide (LPS)-stimulated macrophage inflammation model.

Methods: The in vivo effects of Mag on CIA were studied by inducing CIA in a mouse model using DBA/1J mice followed by treatment with vehicle, methotrexate (MTX, 1 mg/kg/d), and Mag (5 mg/kg/d, 10 mg/kg/d, and 20 mg/kg/d), and the in vitro effects of Mag on macrophages were examined by stimulation of RAW264.7 cells line and peritoneal macrophages (PMs) by LPS in the presence of different concentrations of Mag. Network pharmacology and molecular docking was then performed to predict the the binding ability between Mag and its targets. Inflammatory mediators were assayed by quantitative real-time PCR and enzyme linked immunosorbent assay (ELISA). Signaling pathway changes were subsequently determined by Western blotting and immunohistochemistry (IHC).

Results: In vivo experiments demonstrated that Mag decreased arthritis severity scores, joints destruction, and macrophages infiltration into the synovial tissues of the CIA mice. Network pharmacology analysis revealed that Mag interacted with TNF-α, IL-6, IL-1β, and MCP-1. Consistent with this, analysis of the serum, synovial tissue of the CIA mice, and the supernatant of the cultured RAW264.7 cells and PMs showed that Mag suppressed the expression of TNF-α, IL-6, IL-1β, MCP-1, iNOS, and IFN-β. Furthermore, Mag attenuated the phosphorylation of p65, IκBα, ERK, JNK, and p38 MAPKs in the synovial tissues of the CIA mice and LPS-stimulated RAW 264.7 cells.

Conclusion: Mag may exert anti-arthritic and anti-inflammatory effects by inhibiting the activation of NF-κB and MAPK signaling pathways.

Keywords: magnoflorine, rheumatoid arthritis, collagen-induced arthritis, macrophage, NF-κB/MAPK signaling

Introduction

Rheumatoid arthritis (RA) is a common autoimmune disease and one of the main causes of joint deformity and disability. Epidemiological data show that the incidence of RA in China is 0.28–0.45%[1] and that the prevalence of RA in females is twice as that in males.[2] Clinical symptoms of RA include joint fever, swelling, pain, stiffness, and limited motion and function.[3] The most common treatment drugs for RA patients include disease-modifying anti-rheumatic drugs (DMARDs), nonsteroidal anti-inflammatory drugs (NSAIDs), glucocorticoids, and biological agents. Unfortunately,

Received: 31 January 2023
Accepted: 18 May 2023
Published: 27 May 2023

the application of these therapeutic drugs is limited due to their high costs and/or severe side effects for a majority of RA patients. Thus, there is an urgent need to develop more effective and safer drugs to improve RA outcomes.

Traditional Chinese medicine (TCM) has a long history in the treatment of RA. *Caulis Sinomenii*, recorded in the *Chinese Pharmacopoeia*, is widely used for the treatment of RA and osteoporosis.[4] The major contents of *Caulis Sinomenii* are active alkaloids, such as sinomenine, magnoflorine (Mag), disinomenine, and sinoacutine.[5] As one of the most abundant components, sinomenine has been approved by the National Medical Products Administration of China for treating RA.[6] Sinomenine is extracted from the root and rhizome of Sinomenium acutum plant which grows in forest areas and is mainly found in southwestern, central southern, and eastern China. Recent studies have shown that sinomenine regulated the secretion of inflammatory cytokines and macrophage subsets, and inhibited the activation of the nuclear factor-kappa B (NF-κB) pathway in fibroblast-like synoviocytes (FLS).[7,8] To date, the effects of Mag on macrophage in RA have not been reported.

Mag is isolated from the root, rhizome or stem of the root, rhizome, stem, or bark of several important plants, such as Sinomenium acutum, Berberis kansuensis Schneid, Magnolia officinalis Rehder et E.H. Wilson, and Tinospora cordifolia Miers.[9] As an important quaternary aporphine alkaloid, Mag exerts multiple pharmacological properties, including anti-inflammatory, anti-oxidant, immunomodulatory, and anti-diabetic.[9] Furthermore, researchers have reported that Mag suppressed receptor activators of NF-kB ligand (RANKL)-induced osteoclastogenesis in vitro by inhibiting mitogen-activated protein kinase (MAPK) and NF-κB signaling pathway.[10] Recent evidence has also shown that Mag can alleviate "M1" macrophage-mediated nucleus pulposus cell damage via the high mobility group box protein 1 (HMGB1)-myeloid differentiation primary response gene 88 (MyD88)-NF-κB pathway, indicating its potential role in treating intervertebral disc degeneration.[11] Conversely, Mag may increase immune function through up-regulation of pro-inflammatory markers via activation of the NF-κB, MAPKs, and phosphatidylinositol-3-kinase (PI3K)/Akt signaling pathways in lipopolysaccharide (LPS)-stimulated U937 human macrophages.[12] These findings demonstrate the contradictory effects of Mag on immune response and macrophage.

Although the pathogenesis of RA is still unclear, a growing body of data has demonstrated the important roles of macrophage and inflammatory cytokines in the occurrence and progression of RA. Importantly, macrophages can be divided into classically activated (M1) and alternatively activated (M2) polarized macrophages.[13] M1 macrophages secrete inflammatory cytokines such as interleukin-1β (IL-1β), interleukin-6 (IL-6), and tumor necrosis factor (TNF-α), leading to joint destruction and the apoptosis of parenchymal and mesenchymal cells.[14] Indeed, the infiltration of $CD68^+$ macrophages in synovial tissues is a hallmark of the severity of RA.[15] Therefore, regulation of macrophage phenotype and function remains a key therapeutic target for the treatment of RA.[16] Nevertheless, the function and potential mechanism of Mag in treating RA have yet to be investigated.

In the present study, we evaluated the anti-rheumatoid arthritis effects of Mag on CIA mice in vivo and explored the potential mechanism of Mag in LPS-treated RAW264.7 cells line and peritoneal macrophages in vitro.

Methods and Materials

Chemicals, Reagents, and Antibodies

Mag (purity ≥ 99%) was purchased from Yuanye Biological (Shanghai, China). LPS was purchased from Sigma-Aldrich (St. Louis, MO, USA). Dulbecco's modified Eagle's medium (DMEM) and fetal bovine serum (FBS) were purchased from Thermo Fisher Scientific (Waltham, MA, USA). Bovine type II collagen, complete Freund's adjuvant (CFA), and incomplete Freund's adjuvant (IFA) were procured from Chondrex (Woodinville, WA, USA). The RAW264.7 cells line used in this study was obtained from American Type Culture Collection (ATCC, RM, USA). Enzyme linked immunosorbent assay (ELISA) kits for TNF-α, IL-6, IL-1β, and monocyte chemoattractant protein-1 (MCP-1) were obtained from Meilian (Shanghai, China). TRIzol was purchased from Invitrogen (CA, USA). Reverse transcription kit and quantitative real-time polymerase chain reaction (qRT-PCR) detection kits were purchased from TaKaRa (Shiga, Japan). The primers were synthetized from Ruizhen Biotech (Nanjing, China). Primary antibodies specific to CD68, F4/80, NF-κB pathway sampler kit, MAPK family antibody sampler kit, and phospho-MAPK family antibody sampler kit were obtained from Cell Signaling Technology (Danvers, USA). β-actin antibody was purchased from Boster (Wuhan, China).

Cells Cultures and Treatment

Peritoneal macrophages (PMs) were enriched from DBA/1J mice by flushing the abdominal cavity with 5 mL of pre-cooled phosphate buffered saline (PBS) followed by in vitro culture of peritoneal cells with 90% completed DMEM with 10% FBS. RAW264.7 cells were cultured in 90% completed DMEM and 10% FBS. The PMs and RAW264.7 cells were placed in a humidified atmosphere with 5% CO_2 at 37 °C. PMs and RAW264.7 cells were also pre-treated with vehicle and Mag (25, 50, or 100 μg/mL) for 4 h followed by stimulated with 100 ng/mL LPS for 6 h. The supernatants and adherent cells were harvested for ELISA and qRT-PCR analysis, respectively.

The Collagen-Induced Arthritis Mouse Model and Drug Administration

Six-to-eight-week-old male DBA/1J mice (20 ± 2 g) were purchased from Shanghai SLAC Laboratory Animal and reared in a specific pathogen free (SPF) animal laboratory kept at 21–25 °C with a 12/12h light/dark cycle. The mice were fed complete nutritional pellets and distilled water ad libitum. Ethical approval for this current study was obtained from the Institutional Animal Care and Use Committee at Nanjing University of Chinese Medicine (202207A079). All animal experiments complied with the ARRIVE guidelines and were carried out in accordance with the National Research Council's Guide for the Care and Use of Laboratory Animals.

After an acclimatization period of 1 week, a total of ninety mice were randomly divided into 6 groups (n = 15/group), the unimmunized control group, collagen-induced arthritis (CIA) mice treated with vehicle (dimethyl sulfoxide) group, methotrexate (MTX, 1 mg/kg/d) group, Mag-L (5 mg/kg/d) group, Mag-M (10 mg/kg/d) group, or Mag-H (20 mg/kg/d) group. CIA were induced as previously reported in the literature.[17] Briefly, DBA/1J mice were intradermally injected at the base of the tail with 100μL of bovine type II collagen (2 mg/mL) emulsified with an equal volume of CFA (4 mg/mL) at day 0 and boosted with bovine type II collagen (2 mg/mL) emulsified with an equal volume of IFA at day 21. The CIA mice were i.p. administrated with vehicle, Mag, or MTX daily for two weeks starting from day 35. After the second immunization, the clinical scores of the mice were evaluated according to the following scale (as described previously):[18] grade 0, normal (no swelling); grade 1, swelling and redness of at least 1 joint; grade 2, swelling in>1 joint; grade 3, moderate swelling of the entire paw; grade 4, paw deformity and/or ankylosis. Each paw was graded with a score of 0 to 4, and each mouse was thus evaluated on a scale of 0 to 16. Two independent observers assessed the clinical scores under blinded conditions.

All the mice were euthanized under isoflurane anesthesia at day 49. The right ankle joints and spleen were then fixed in 10% neutral buffered formalin for pathological and immunohistochemical examinations. The left ankle joints and PMs were used for mRNA expression analysis.

Micro-Computed Tomography (Micro-CT) Analysis

To obtain focal bone destruction in the ankles, we evaluated the three-dimensional (3-D) reconstructions of ankle joints by micro-CT after two weeks of drug intervention, and the Micro-CT exams were performed as previously reported in the literature.[19] The mice were anesthetized with isoflurane and the right hind paws were fixed. Each mouse was then subjected to Quantum GX micro-CT analysis (Quantum GX, PerkinElmer, Hopkinton, MA, USA). The scanning parameters were set to 90 kV and 80 μA. Finally, the CT images were visualized via a 3-D Viewer, an existing software program within the Quantum GX, and all the captured pictures were reconstructed and realigned in 3-D.

Histology Analysis

The right ankle joints and spleens were fixed in 10% neutral buffered formalin overnight followed by decalcification in EDTA decalcified solution for 2 d, as described elsewhere.[7] After dehydration, the ankle joints and spleen embedded in paraffin were cut into 4 to 5 μm slices and stained with hematoxylin-eosin (H&E). Pathological changes of the joints and spleens were then observed and photographed by light microscope. Briefly, joints were scored based on synovial tissue proliferation, pannus formation, inflammatory cell infiltration, and bone erosion. Pathological scoring of the spleens was performed according to the number of germinal centers in the spleen, marginal zone hyperplasia, and red pulp hyperemia. Histological changes were evaluated blindly by two examiners as described previously.[20]

Screening of the Structures and Targets of Mag

The TCM Systems Pharmacology Database and Analysis Platform (TCMSP; https://tcmspw.com/tcmsp.php)[21] and BATMAN-TCM (http//bionet.ncpsb.org/batman-tcm)[22] were used to obtain the biochemical properties of Mag, including its absorption, distribution, metabolism, and excretion (ADME) parameters. The 2-D and 3-D structures of Mag were downloaded from the Pubchem (https://pubchem.ncbi.nlm.nih.gov) database.[23] Finally, all the names of Mag targets were switched to their corresponding gene names using the UniProt database (www.uniprot.org).[24] Cytoscape software 3.7.2 (https://cytoscape.org) was then used to construct a Mag-target network diagram.

Identification of RA-Related Targets and Overlapping Targets of Mag Treatment on RA

The keywords "rheumatoid arthritis" was used to search for RA-related targets through the following databases: Online Mendelian Inheritance in Man (OMIM; https://omim.org),[25] GeneCards (www.genecards.org),[26] and DrugBank (https://go.drugbank.com).[27] We set "relevance score" ≥ 30% as the cutoff to select targets from the GeneCards database. All targets were then merged from the above three databases with duplicate targets removed. Finally, the names of RA-related targets were switched to their gene names using the UniProt database. The targets of Mag and RA-related targets were then imported into Venny in order to obtain targets shared by Mag and RA (Bardou, Mariette, Escudié, Djemiel, and Klopp, 2014; version 2.1.0, http://bioinformatics.psb.ugent.be/webtools/Venn) (a professional tool for producing Venn diagrams).[28]

Molecular Docking

We obtained the 3-D structures of TNF-α, IL-6, IL-1β, and MCP-1 from protein the data bank (PDB) database (https://www.rcsb.org/),[29] and we defined the TNF-α, IL-6, IL-1β, and MCP-1 targets were defined as macromolecules. Subsequently, the macromolecules were modified, including ligand and water removal, and hydrogen addition by PyMol software.[30] Furthermore, we used AutoDockTools-1.5.6 software to carry out molecular docking and obtained the targets for the above as well as and Mag-related information. The smaller binding energy of macromolecules and Mag means an easier connection between targets and ingredients. Ultimately, these results were visualized by PyMol software.

Flow Cytometry Assay

The F4/80 molecule has been recognized as a unique marker of murine macrophages.[31] We therefore applied flow cytometry assay to detect the percentage of $F4/80^+$ PMs in peritoneal cells as previously reported in the literature.[7] The cultured peritoneal cells were digested by 1 mL trypsin and resuspended in cold PBS. Next, the PMs were stained with allophycocyanin (APC)-F4/80 antibody or isotype control in 4 °C in the dark for 30 min. The following gating strategy was then applied: First, the main population was defined by forward scatter (FSC) and side scatter (SCC). Then, the cells of this FSC/SSC gate were evaluated for expression of F4/80. After this, the proportion of $F4/80^+$ PMs was detected by BD FACS Canto II Flow Cytometer (BD, NY, USA).

Cell Viability

The RAW264.7 cells were collected into 96-well plates at a density of 5×10^3 per well and cultured with complete medium up to 80% of cells density. Subsequently, the RAW264.7 cells were treated with different concentrations of Mag (0, 1, 5, 10, 25, 50, 100, 200, 500, and 1000 μg/mL) for 24 h followed by culture with 10 μL of Cell Counting Kit-8 (CCK-8) for another 2 h. The optical density (OD) with 450 nm light was then determined using BioRad 3350 microplate reader (BioRad, Hercules, CA). Results are shown as percentage of control, as previously reported in the literature.[32]

RNA Isolation and qRT-PCR

Total RNA in ankle joints and macrophages were both isolated using TRIzol reagent and transcribed to cDNA using PrimeScript™ RT reagent kit according to the manufacturer's instructions. The expression levels of TNF-α, IL-6, IL-1β, MCP-1, inducible nitric oxide synthase (iNOS), and interferon-beta (IFN-β) were measured by SYBR Green Real time PCR Master Mix and tested by Applied Biosystems 7500 Real-Time PCR System (Thermo Fisher Scientific, Waltham,

MA, USA). Relative gene expression levels were then calculated using the $2^{-\Delta\Delta Ct}$ formula[33] and normalized to the expression of glyceraldehyde-3-phosphate dehydrogenase (GAPDH). Each experiment was performed in triplicate. The primer sequences are shown in Table 1.

ELISA

The orbital blood from the mice were placed at room temperature (RT) for more than 30 min and centrifuged at 3500 g for 15 min to obtain the serum. Cell supernatant from the PMs and RAW264.7 cells were also collected by centrifugation at 12,000 g for 5 min. The concentration of IL-1β, MCP-1, IL-6, and TNF-α in the serum and supernatant were determined using the corresponding commercial ELISA kits according to the manufacturer's instructions. Briefly, all materials and prepared reagents were equilibrated to RT prior to use. Then, the standards and samples were diluted to the desired concentrations in blocking solution, and 50 μL per well was added to the ELISA plate along with 100 μL horseradish peroxidase-labeled antibody (TNF-α or IL-6 or IL-1β or MCP-1) and incubated 1 h at 37°C. Next, the samples were washed 5 times with PBS/Tween. 6 mL of tetramethylbenzidine (TMB) Reagent A was then mixed with 6 mL of TMB Reagent B immediately prior to use, and 100 μL were transferred into each well. After this, the samples were incubated at 37°C 15 min for color development. To stop the color reaction, 50 μL of TMB Stop Solution was then added. Finally, the absorbance at 450 nm was recorded using on a BioRad 3350 microplate reader within 15 min of stopping the reaction.[34]

Immunohistochemistry Staining

The slices from each ankle joint were incubated with 5% goat serum for 30 min at RT. After rinsing and heat-induced epitope retrieval, the sections were then incubated with anti-F4/80(1:200), anti-CD68(1:300), anti-phospho-p65 (1:400), anti-phospho-inhibitory subunit of NF kappa b alpha (IκBα) (1:200), anti-phospho-extracellular regulating kinase (ERK)1/2 (1:400), and anti-phospho-p38 MAPK (1:800) primary antibodies overnight at 4 °C, followed by blocking of endogen peroxidase with 1.5% H_2O_2 for 10 min. Then, the slices were incubated with secondary antibody goat-anti-rabbit IgG horseradish peroxidase (HRP) at 37 °C for 30 min. The sections were subsequently visualized with DAB (3,3′-diaminobenzidine), and the Image J software (National Institutes of Health, Bethesda, MD, USA) was used to measure the average optical density (AOD) of anti-F4/80, anti-CD68, anti-phospho-p65, anti-phospho-IκBα, anti-phospho-ERK1/2, and anti-phospho-p38 MAPK.[34]

Western Blotting

The RAW264.7 cells were seeded into 6-well plates at a density of 1.5×10^6 per well, and the cells were pretreated with Mag for 1 h followed by stimulation with 100 ng/mL LPS for 1 h. The cells were then lysed with pre-cool radioimmunoprecipitation assay (RIPA) lysis buffer that contained protease inhibitor as well as phosphatase inhibitor, and the concentration of proteins were then detected using the bicinchoninic acid (BCA) method.[35] Next, the samples (30 μg) were separated by sodium dodecyl sulfate-polyacrylamide gel electrophoresis (SDS-PAGE) and then transferred to a polyvinylidene fluoride (PVDF) membrane. After being blocked in tris-buffered saline plus Tween 20 (TBST) with 5% bovine serum albumin (BSA) for 1 h at RT, the membranes were then incubated with primary antibodies, including

Table 1 Primer Sequences for qRT-PCR

Gene	Forward Primer	Reward Primer
TNF-α	CCCTCACACTCAGATCATCTTCT	GCTACGACGTGGGCTACAG
IL-6	TAGTCCTTCCTACCCCAATTTCC	TTGGTCCTTAGCCACTCCTTC
IL-1β	GAAATGCCACCTTTTGACAGTG	CTGGATGCTCTCATCAGGACA
MCP-1	TTAAAAACCTGGATCGGAACCAA	GCATTAGCTTCAGATTTACGGGT
iNOS	ACATCGACCCGTCCACAGTAT	CAGAGGGGTAGGCTTGTCTC
IFN-β	CAGCTCCAAGAAAGGACGAAC	GGCAGTGTAACTCTTCTGCAT
GAPDH	TGAGGCCGGTGCTGAGTATGT	CAGTCTTCTGGGTGGCAGTGAT

p38 MAPK (1:1000), phospho-p38 MAPK (1:1000), JNK (1:1000), phospho-JNK (1:1000), ERK1/2 (1:1000), phospho-ERK1/2 (1:2000), p65 (1:1000), phospho-p65 (1:1000), IκBα (1:1000), and phospho-IκBα (1:1000) overnight at 4°C. The membranes were then washed three times using TBST and incubated with appropriate anti-rabbit IgG (1:3000) or anti-mouse IgG (1:3000) secondary antibody for 2 h at RT. After this, the expression levels of each protein were performed by enhanced chemiluminescence (ECL, Millipore). A Tanon 4600 chemiluminescence imaging analysis system (Shanghai, China) was used to record the images, and Image J software to calculate the density of the proteins.[34]

Statistical Analysis

Statistical analysis was performed using GraphPad Prism (Version 8). All experimental data were expressed as mean ± standard deviation (SD), mean ± standard error of the mean (SEM), or medians (interquartile ranges [IQR]). Normality of variables was checked with the Shapiro–Wilks test, and the homogeneity of variance was examined by Levene's test. One-way analysis of variance (ANOVA) followed by Tukey's post hoc test (normal distributed data) or Kruskal–Wallis test (non-normal distributed data) were used for multiple group comparisons. For all tests, $P < 0.05$ was considered to indicate statistically significant results.

Results

Mag Alleviates the Clinical Symptoms of Arthritis and Articular Bone Damage in CIA Mice

To determine the in vivo effect of Mag on RA, we first established the mice CIA model. After the onset of arthritis on day 35, mice were then treated with vehicle, MTX, or different doses of Mag (5 mg/kg/d, 10 mg/kg/d, or 20 mg/kg/d), respectively. After immunization, the CIA mice displayed progressively paw and joint swelling compared to the control group from day 25, indicating that the CIA model had been successfully established. After the second immunization, the mice were scored for arthritis every 4 days. About 1 week after booster immunization, the joints of the CIA mice had become swollen, and they reached their peak swelling on the 33rd day (Figure 1A and B). After 2 weeks of administration, there was an obvious difference between the MTX and Mag groups compared to the Model group. As displayed in Figure 1B, MTX (a positive control drug) significantly inhibited joints swelling and arthritis scores of the CIA mice from day 41 to day 49. Moreover, after treatment with Mag, the arthritis scores of the CIA mice decreased. Compared to the Model group (8.85±2.15), the arthritis scores of mice in the Model+Mag-M (6.31±0.75) and Model +Mag-H group (6.46±1.27) significantly decreased on the 37th day (both $P < 0.01$). There was also significant difference between Model+Mag-L group and Model group on the 41st day (6.77±1.42 vs 9.31±2.29, $P < 0.05$) and on the 49th day (5.62±1.76 vs 8.54±1.90, $P < 0.01$), respectively. Furthermore, higher doses of Mag (Mag-M and Mag-H) significantly reduced joints swelling and arthritis scores of the CIA mice from day 41 to day 49 (all $P < 0.001$).

To evaluate bone destruction, we performed a 3-D reconstruction of the ankle joints in mice by micro-CT. This Micro-CT examination as well as 3-D imaging analysis revealed that the articular surfaces of the mice in control group were smooth, and the structural integrity of their articular bones was undamaged (Figure 1C). Conversely, the joint structures of the CIA mice in the Model group were seriously damaged (Figure 1C). After MTX or Mag treatment, however, we observed that the articular bone damage was reduced compared to the Model group (Figure 1C).

Mag Alleviates Inflammation and Bone Damage in Ankle Joints and Impairment in Spleens of CIA Mice

We next examined the histological changes in the ankle joints and spleens of the Mag-treated CIA mice by H&E staining. As shown in Figure 2A, compared to the control group, the CIA mice displayed synovial tissue hyperplasia, pannus formation, inflammatory cells infiltration into the synovium, articular cartilage erosion, and bone destruction. After Mag or MTX treatment, however, these pathological characteristics improved. In Figure 2B, the histopathological scores show that different doses of Mag significantly inhibited the hyperplasia of joint synovial tissue (all $P < 0.01$), pannus formation (all $P < 0.001$), inflammation (all $P < 0.001$), and the destruction of articular cartilage (all $P < 0.05$).

As the largest peripheral immune organ, the spleen contains a great number of lymphocytes and macrophages, and abnormal splenic function is closely related to development of RA.[20] As shown in Figure 2C, the increase in the germinal center, infiltration of inflammatory cells, and hyperplasia of the marginal zone in the CIA mice were obvious compared to the control group. However, when the CIA mice were treated with Mag or MTX, the structural damage of the spleen was relieved. As shown in Figure 2D, the pathological scoring for the germinal center (all $P < 0.001$), the proliferation of red pulp (all $P < 0.001$), and the expansion of the marginal zone (all $P < 0.001$) were reduced in the Mag or MTX groups. Collectively, these results suggest that Mag reduced the inflammation and local immune response of the CIA mice.

Mag Attenuates the Pro-Inflammatory Macrophages Infiltration into the Ankle Joints of CIA Mice

As mentioned above, the F4/80 molecule has been identified as a unique marker of mouse macrophages.[31] Moreover, CD68 has commonly been used as a marker for the identification of synovial macrophages.[36] As shown in Figure 3A and Figure 3, the AOD of macrophages stained by F4/80 in synovium increased markedly in the Model group compared to

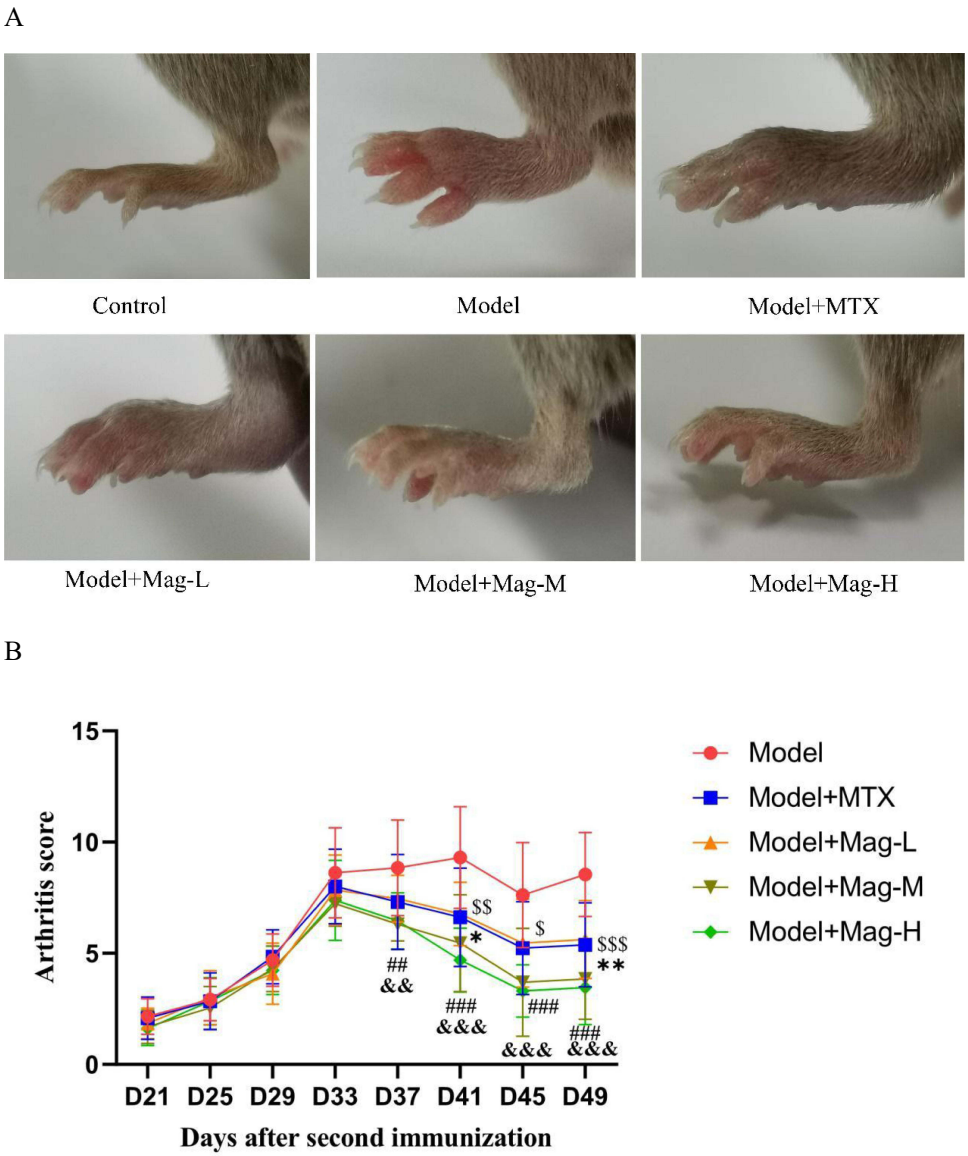

Figure 1 Continued.

C

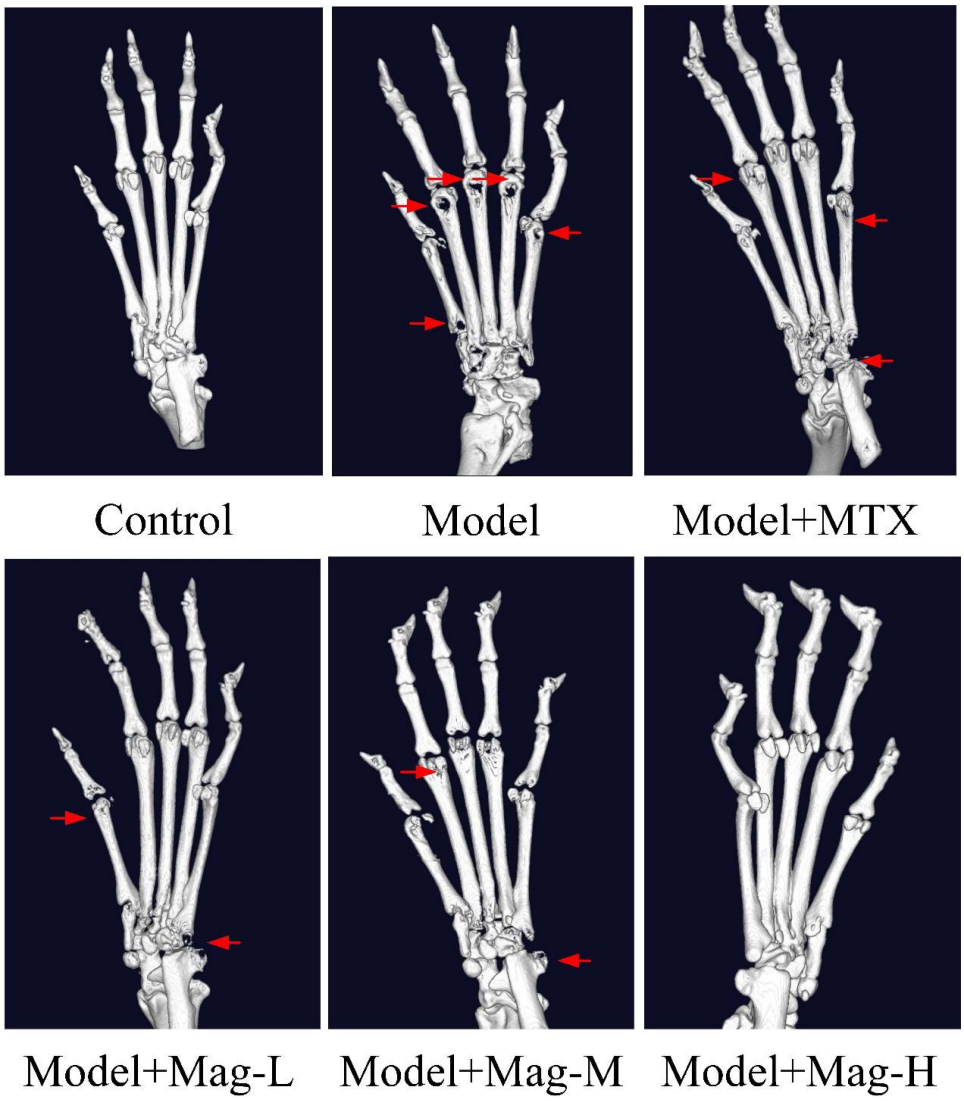

Figure 1 The effects of Mag on severity of arthritis in CIA mice. (**A**) Joint swelling of mice in each group. (**B**) Arthritis scores of mice in each group (n = 15). D37, $^{\#\#}$p<0.01, Model+Mag-M vs Model group; $^{\&\&}$p<0.01 Model+Mag-H vs Model group; D41, $^{\$\$}$p<0.01, Model+MTX vs Model group; *p<0.05, Model+Mag-L vs Model group; $^{\#\#\#}$p<0.001, Model+Mag-M vs Model group; $^{\&\&\&}$p<0.001, Model+Mag-H vs Model group; D45, $^{\$}$p<0.05, Model+MTX vs Model group; $^{\#\#\#}$p<0.001, Model+Mag-M vs Model group; $^{\&\&\&}$p<0.001, Model+Mag-H vs Model group; D49, $^{\$\$\$}$p<0.001, Model+MTX vs Model group; **p<0.01, Model+Mag-L vs Model group; $^{\#\#\#}$p<0.001, Model+Mag-M vs Model group; $^{\&\&\&}$p<0.001, Model+Mag-H vs Model group. (**C**) Representative Micro-CT 3-D reconstructed images of ankle joints in mice (n = 15). The articular damage was indicated by the red arrows. Control group, normal mice; Model group, CIA mice models; Model+MTX group, methotrexate-treated mice (1mg/kg/d)+CIA; Model+Mag-L group, mice with magnoflorine treatment (5mg/kg/d)+CIA; Model+Mag-M group, mice with magnoflorine treatment (10mg/kg/d)+CIA; Model+Mag-H group, mice with magnoflorine treatment (20mg/kg/d)+CIA.

Abbreviations: CIA, collagen induced arthritis; Mag, magnoflorine; Micro-CT, micro-computed tomography.

the control group (0.58±0.01 vs 0.19±0.01, *P*<0.001). After treatment with different doses of Mag, the expression of F4/80 in ankle synovial tissue were also lower than in the CIA group (0.37±0.01, 0.36±0.02, 0.29±0.03 vs 0.58±0.01, all P<0.001) (Figure 3A and Figure 3), indicating that Mag may have inhibited the infiltration of macrophages. Furthermore, we found that the infiltration of CD68-positive cells in the synovium was enhanced in the Model group (0.54±0.01 vs 0.26±0.02, *P*<0.001). Nevertheless, Mag-M, Mag-H or MTX treatment evidently diminished the CD68 positive cells (0.36±0.03, 0.26±0.04, 0.32±0.002 vs 0.54±0.01, all P<0.001). These data suggest that Mag ameliorated the infiltration of macrophages into the ankle joints of CIA mice.

Network Pharmacology and Molecular Docking Predicted Potential Key Proteins Targeted by Mag in RA Treatment

Network pharmacology and molecular docking were performed to predict potential target of Mag in RA treatment. Initially, we queried the biological characteristics of Mag from the TCMSP database. Mag has a molecular weight (MW) of 342.42 $gmol^{-1}$, an oral bioavailability (OB) of 26.69%, and a drug likeness (DL) of 0.55. The 2-D and 3-D structures of Mag are shown in Figure 4A and Figure 4. In total, we found 21 targets of Mag. In addition, the targets together with a Mag network diagram were constructed by Cytoscape 3.7.2 software, as shown in Figure 4C.

Next, we used the keywords "rheumatoid arthritis" to retrieve RA-related targets from the OMIM, Genecards, and Drugbank databases, which returned 513, 98, and 534 RA-related targets, respectively. A total of 738 RA targets were remained after screening and de-duplicating. We then introduced the 21 chemical targets of Mag and 738 RA-related targets into Venny 2.1.0 and were left with 6 overlapping targets (Figure 4D): acetylcholinesterase (ACHE), carbonic anhydrase II (CA2), pregnane X receptor (PXR), prostaglandin G/H synthase 2 (PTGS2), prostaglandin G/H synthase 2 (PTGS1), and retinoic acid receptor RXR-alpha (RXRA).

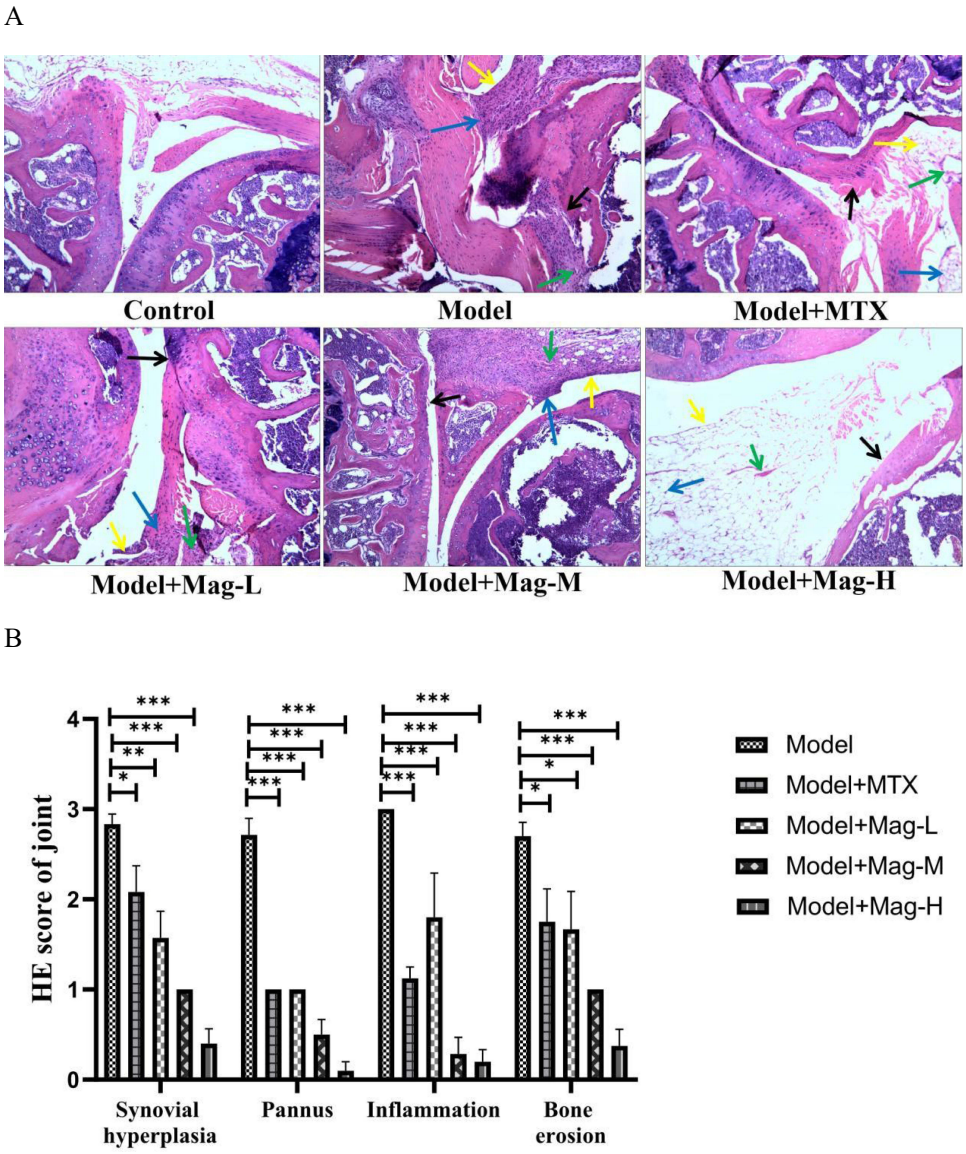

Figure 2 Continued.

C

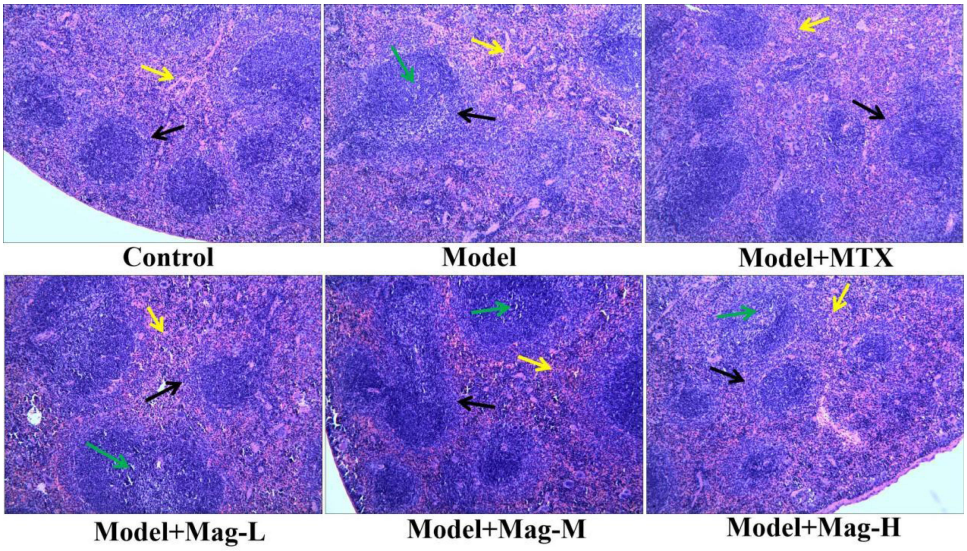

D

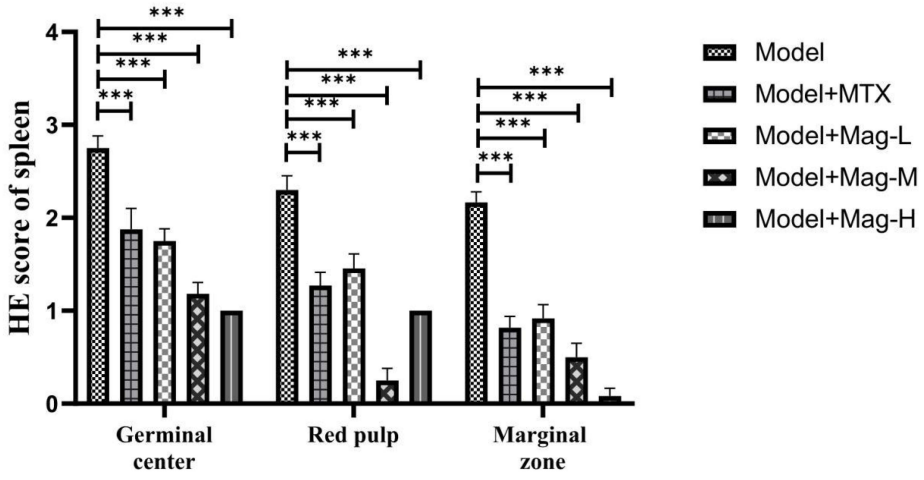

Figure 2 The effects of Mag on the histopathological changes in ankle joints and spleens in CIA mice. (**A**) Representative photomicrographs of HE-stained histological sections (magnification, ×100) of the ankle joints are shown. The histology sections of the ankle joints include the synovial hyperplasia (yellow arrow), pannus formation (green arrow), and infiltration of inflammatory cells (blue arrow), as well as bone erosion (black arrow). (**B**) Histopathological scores of ankle joints in each group (n = 15). (**C**) Representative photomicrographs of HE-stained histological sections (magnification, ×100) of the spleen are shown. The histology section of the spleen include the germinal center (green arrow), red pulp (yellow arrow), and marginal zone (black arrow). (**D**) Histopathological scores of spleens in each group (n = 15). *p<0.05, **p<0.01, ***p<0.001 (one-way ANOVA with Tukey's post hoc test).
Abbreviations: CIA, collagen induced arthritis; HE, hematoxylin-eosin; Mag, magnoflorine.

Finally, we applied the molecular docking to assess the binding ability between inflammatory molecules targets and Mag. The structures of TNF-α, IL-6, IL-1β, and MCP-1 were obtained from the PDB database. We observed that the binding-ability of TNF-α-Mag (−2.91 kcal/Mol), IL-6-Mag (−2.28 kcal/Mol), IL-1β-Mag (−2.6 kcal/Mol), and MCP-1-Mag (−3.53 kcal/Mol) were all less than −2.0 kcal/Mol. The smaller the connection energy is, the easier the connection between the target and the combination is. Among the above inflammatory molecules, MCP-1-Mag had the lowest value, at −3.53 kJ/mol-1. These molecular docking results show that Mag has good binding ability with TNF-α, IL-6, IL-1β, and MCP-1 (Figure 4E).

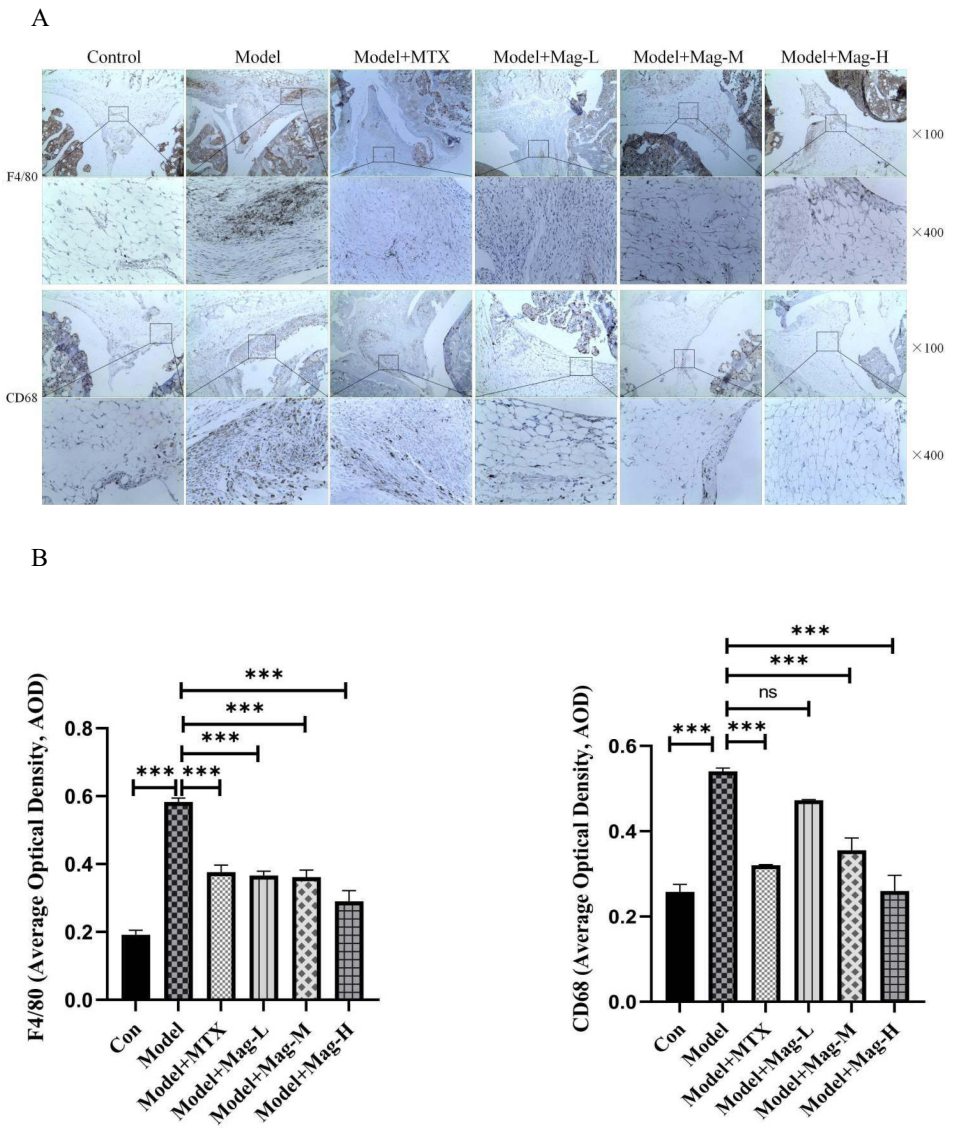

Figure 3 The effects of Mag on the infiltration of macrophages into the ankle joints of CIA mice. IHC analysis was used to evaluate the expression of F4/80 and CD68 in the ankle joints. F4/80 is as a marker of total macrophages. CD68 was chosen for marking pro-inflammatory macrophages. (**A**) Representative photomicrographs of F4/80 and CD68 in ankle joints stained by IHC (magnification, ×100, ×400). (**B**) The average optical density of F4/80 and CD68 in the synovial tissues of the mice in each group were quantitatively analyzed by Image J software (n = 15). ***P<0.001 (one-way ANOVA with Tukey's post hoc test).
Abbreviations: CIA, collagen induced arthritis; Mag, magnoflorine; IHC, immunohistochemistry; NS, no significance.

Mag Suppresses Expression of Inflammatory Cytokines and Chemokines in CIA Mice

The above bioinformatics analysis led us to further experimentally validate whether Mag regulates the expression of these inflammatory mediators. First, the concentrations of TNF-α, IL-6, IL-1β, and MCP-1 in serum were assayed by ELISA. As shown in Figure 5A, the levels of TNF-α (685.5±12.74 vs 401.8±19.15 pg/mL, P<0.001), IL-6 (111.5±7.62 vs 49.42±1.63 pg/mL, P<0.001), IL-1β (78.48±4.69 vs 47.13±1.29 pg/mL, P<0.001), and MCP-1(28.8±1.57 vs 16.14 ±0.65 pg/mL, P<0.001) in the serum of the CIA mice were significantly higher compared to the control group, respectively. However, Mag-L, Mag-M, Mag-H, or MTX resulted in lower levels of TNF-α (463.4±24.84, 444.6 ±33.64, 391.9±11.35, 419.9±20.16, vs 685.5±12.74 pg/mL, all P<0.001), IL-6 (79.62±4.6, 71.24±5.07, 59.02±1.48, 74.75±3.74, vs 111.5±7.62 pg/mL, all P<0.001), IL-1β (61.89±1.03, 54.16±4.34, 42.27±1.3, 50.76±7.19, vs 78.48±4.69 pg/mL, all P<0.001), and MCP-1 (22.99±2.22, 20.64±1.2, 17.84±0.89, 20.96±2.23, vs 28.8±1.57 pg/mL, all P<0.001).

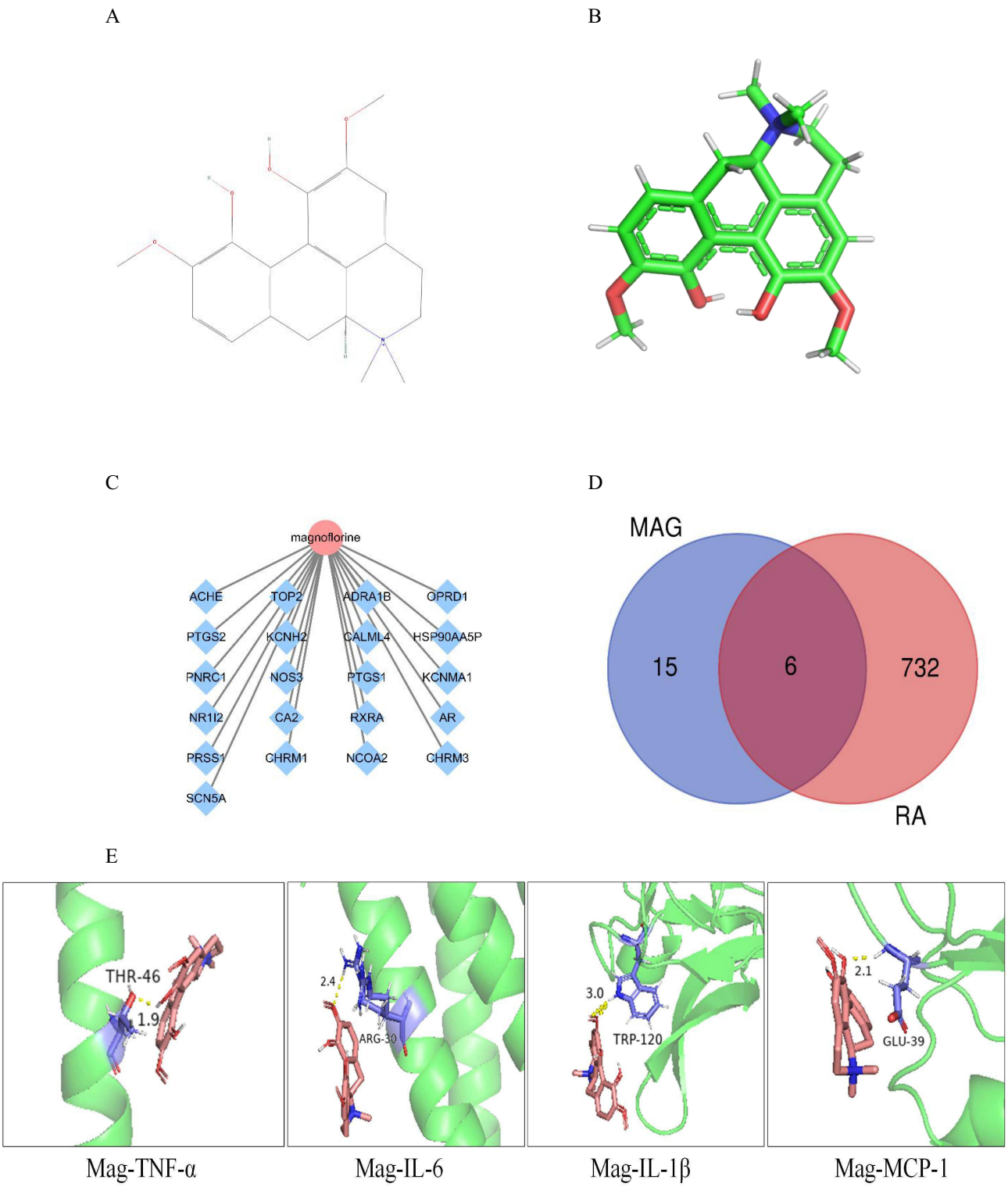

Figure 4 Network pharmacology and molecular docking predicted potential key proteins targeted by Mag in RA treatment. (**A**) The 2-D structure of Mag. (**B**) The 3-D structure of Mag. (**C**) Mag-target network. Mag comprises 21 target nodes, and the gene targets are shown as blue diamonds. (**D**) The overlapping targets of Mag and RA. (**E**) The molecular docking of the TNF-α, IL-6, IL-1β, MCP-1 targets and Mag.
Abbreviations: Mag, magnoflorine; 3-D, three-dimensional; 2-D, two-dimensional.

Next, the expression levels of TNF-α, IL-6, IL-1β, MCP-1, iNOS, and IFN-β mRNA in ankle joints were evaluated by qRT-PCR. As shown in Figure 5B, the qRT-PCR analysis showed that the expression levels of the TNF-α (34.1-fold), IL-6 (151.1-fold), IL-1β (49.3-fold), MCP-1(178.1-fold), iNOS (12.47-fold), and IFN-β (33.74-fold) in ankle joints in the

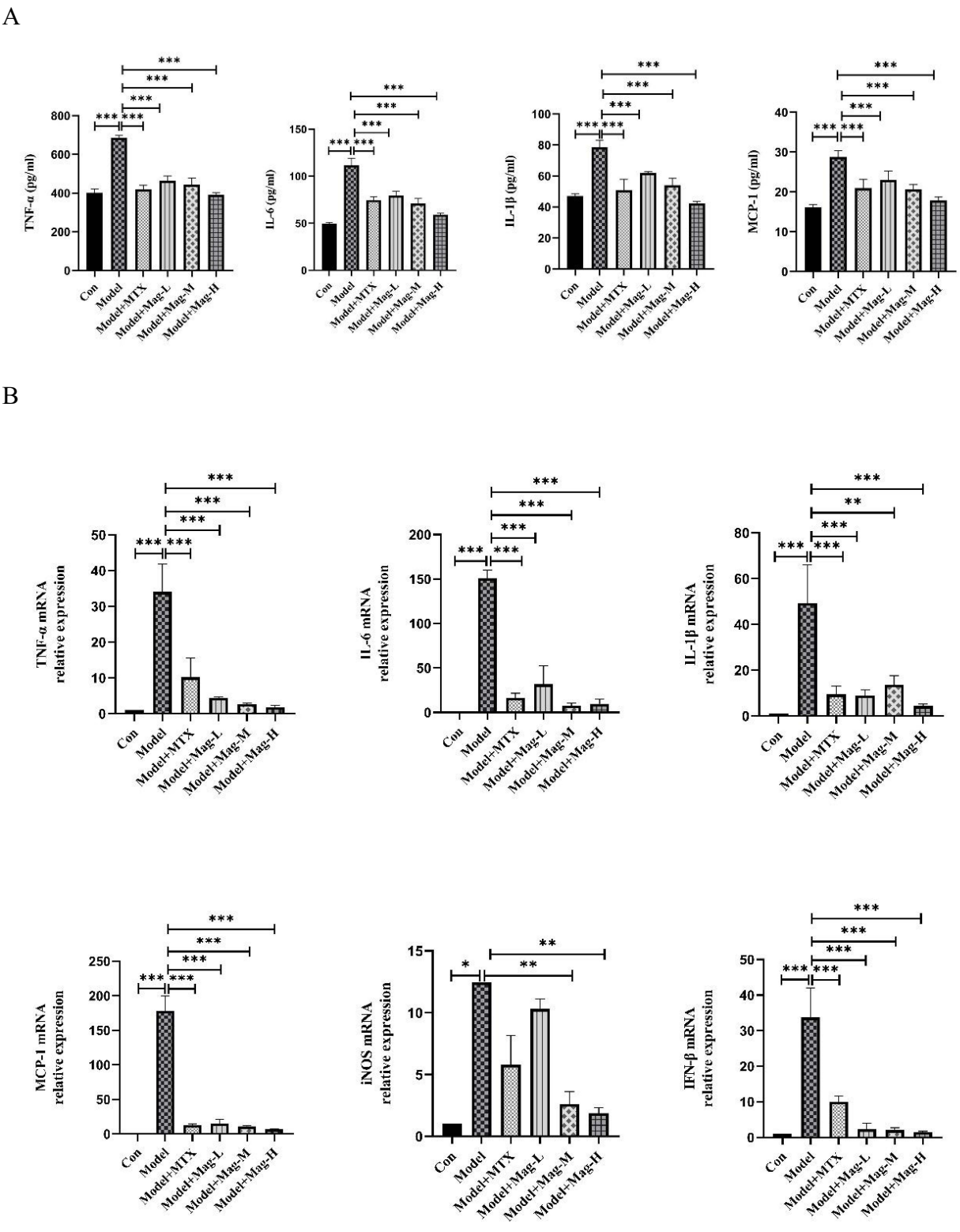

Figure 5 Continued.

C

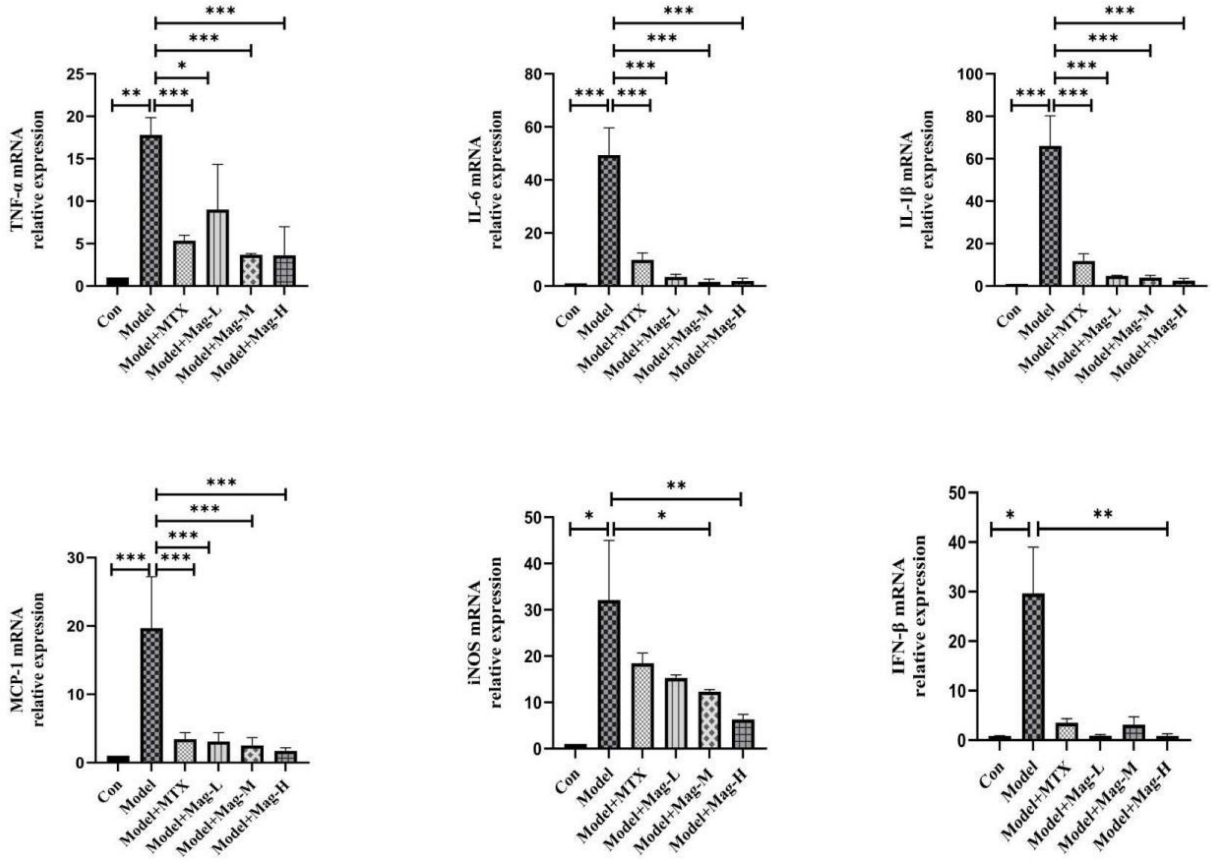

Figure 5 The effects of Mag on the expression of inflammatory cytokines and chemokines in CIA mice. (**A**) ELISA was used to detect the concentrations of TNF-α, IL-6, IL-1β, and MCP-1 in the serum of mice in each group. (**B**) qRT-PCR was performed to investigate the mRNA expression of TNF-α, IL-6, IL-1β, MCP-1, iNOS, and IFN-β in the synovial tissues of the mice in each group. (**C**) qRT-PCR was performed to investigate the mRNA expression of TNF-α, IL-6, IL-1β, MCP-1, iNOS, and IFN-β in the peritoneal macrophages of CIA mice. Data in (**A**–**C**) are representative of at least three repetitions. **P*<0.05, ***P*<0.01, ****P*<0.001 (one-way ANOVA with Tukey's post hoc test or Kruskal–Wallis test).

Abbreviations: Mag, magnoflorine; ELISA, enzyme linked immunosorbent assay; TNF-α, tumor necrosis factor; IL-6, interleukin-6; IL-1β, interleukin-1β; MCP-1, monocyte chemoattractant protein-1; iNOS, inducible nitric oxide synthase; IFN-β, interferon-beta; qRT-PCR, Quantitative Real-Time PCR; CIA, collagen induced arthritis.

CIA mice were dramatically higher compared to the control group. However, different doses of Mag or MTX significantly down-regulated the expression of the TNF-α (4.46-fold, 2.72-fold, 1.82-fold, 10.2-fold vs 34.1-fold, all $P<0.001$), IL-6 (31.76-fold, 7.54-fold, 9.66-fold, 16.37-fold vs 151.1-fold, all $P<0.001$), IL-1β (8.87-fold, 13.65-fold, 4.40-fold, 9.49-fold vs 49.3-fold, all $P<0.01$), MCP-1 (15.26-fold, 11.14-fold, 7.08-fold, 12.88-fold, vs 178.1-fold, all $P<0.001$), and IFN-β (2.37-fold, 2.10-fold, 1.51-fold, 10.03-fold, vs 33.74-fold, all $P<0.001$). Although Mag-L and MTX had no obvious effect on the mRNA expression of iNOS, treatment with Mag-M (2.63-fold vs 12.47-fold, $P < 0.01$) and Mag-H (1.89-fold vs 12.47-fold, $P < 0.01$) appeared to decrease the expression of iNOS mRNA significantly.

Finally, qRT-PCR was also used to determine the expression of inflammatory cytokines and chemokines in the PMs of CIA mice. As shown in Figure 5C, these qRT-PCR results revealed that the mRNA expression levels of TNF-α (17.8-fold, $P < 0.01$), IL-6 (49.39-fold, $P < 0.001$), IL-1β (66.06-fold, $P < 0.001$), MCP-1(19.69-fold, $P < 0.001$), iNOS (32.11-fold, $P < 0.05$), and IFN-β (31.02-fold, $P < 0.05$) in the PMs of CIA mice were substantially higher compared to the control group. However, different doses of Mag significantly inhibited the expression of the TNF-α (9.02-fold, 3.67-fold, 3.61-fold vs 17.8-fold, all $P < 0.05$), IL-6 (3.46-fold, 1.54-fold, 1.88-fold, vs 49.39-fold, all $P < 0.001$), IL-1β (4.79-fold, 3.95-fold, 2.54-fold, vs 66.06-fold, all $P < 0.001$), and MCP-1 (3.09-fold, 2.52-fold, 1.71-fold vs 19.69-fold, all $P < 0.001$). Moreover, Mag-H markedly inhibited the expression of IFN-β (0.48-fold, vs 31.02-fold,

$P < 0.01$). Although Mag-L and MTX had no obvious effect on the mRNA expression of iNOS, treatment with Mag-M (12.3-fold vs 32.11-fold) and Mag-H (6.3-fold vs 32.11-fold) appeared to decrease the expression of iNOS mRNA significantly (both $P < 0.05$).

Mag Reduces the Expression of Pro-Inflammatory Cytokines, Mediators, and Chemokines in LPS-Induced RAW264.7 Cells

To determinate the cytotoxic activity of Mag, we examined the effect of Mag on RAW264.7 cells. As displayed in Figure 6A, CCK-8 assay showed that Mag with low concentrations (1, 5, 10, 25, 50, 100, and 200 μg/mL) had minimal influence on the viability of RAW264.7 cells. Only the high concentrations of Mag (500 and 1000 μg/mL) appeared to inhibit the viability of the RAW264.7 cells (both $P<0.001$).

To identify the anti-inflammatory activity of Mag, we first determined the mRNA levels of typical pro-inflammatory cytokines, chemokines, and mediators. qRT-PCR analysis showed that LPS dramatically stimulated the expression levels of TNF-α, IL-6, IL-1β, MCP-1, iNOS, and IFN-β mRNA in the RAW264.7 cells (all $P<0.001$) (Figure 6B). However, treatment with Mag resulted in significant suppression of the mRNA expression of these pro-inflammatory cytokines, chemokines, and mediators. In addition, we observed that different doses of Mag reduced the expression of TNF-α (17.95-fold, 14.02-fold, 15.40-fold, vs 21.61-fold), IL-6 (69.67-fold, 54.65-fold, 31.15-fold, vs 96.51-fold), IL-1β (4515-fold, 2321-fold, 1853-fold, vs 8045-fold), MCP-1(43.82-fold, 28.72-fold, 24.97-fold, vs 74.17-fold), iNOS (671.4-fold, 436.5-fold, 373.7-fold, vs 1269-fold), and IFN-β (235.3-fold, 174.3-fold, 150.1-fold, vs 303.0-fold) mRNA.

We also determined the concentrations of TNF-α, IL-6, IL-1β, and MCP-1 in the supernatant of LPS-stimulated RAW264.7 cells that were pre-treated with Mag. As presented in Figure 6C and consistent with the mRNA results, we observed that the concentrations of TNF-α (4415±58.33 vs 135.6±1.57pg/mL, $P<0.001$), IL-6 (608.4±104.2 vs 25.87 ±0.81pg/mL, $P<0.001$), IL-1β (90.50(82.05~96.68) vs 31.12(28.60~41.04)pg/mL, $P<0.05$), and MCP-1 (815.5±52.19 vs 21.43±0.67pg/mL, $P<0.001$) increased markedly in the LPS-treated group. However, the RAW264.7 cells treated with varying concentration of Mag showed significant reduced expression of TNF-α (2818±64.43, 2316±95.85, 1514±82.50, vs 4415±58.33 pg/mL, all $P<0.001$), IL-6 (284.8±48.29, 112.8±40.22, 92.24±6.10, vs 608.4±104.2 pg/mL, all $P<0.01$), and MCP-1 (387.6±81.49, 339.3±28.62, 107.9±31.99, vs 815.5±52.19 pg/mL, all $P<0.01$). Different doses of Mag had no obvious effects on the concentration of IL-1β (70.77 (56.64~84.91), 43.35 (42.19~44.51), 65.68 (61.73~69.63), vs 90.50 (82.05~96.68) pg/mL, all $P > 0.05$) in LPS-treated group.

Mag Inhibits the Expression of Pro-Inflammatory Cytokines, Mediators, and Chemokines in LPS-Induced PMs

We next examined the effects of Mag on PMs. In this study, PMs were isolated from the peritoneal cavity of DBA1/J mice. The purity of the PMs was measured by flow cytometry. We found that the percentage of peritoneal adherent cells expressing F4/80 was above 90% (Figure 7A).

qRT-PCR analysis showed that LPS significantly induced the expression of TNF-α, IL-6, IL-1β, MCP-1, iNOS, and IFN-β mRNA in the PMs. However, Mag abated the mRNA expression of IL-1β (12.09-fold, 14.09-fold, 13.38-fold, vs 24.45-fold, all $P<0.05$), IFN-β (8.91-fold, 5.97-fold, 3.43-fold, vs 35.33-fold, all $P<0.01$), MCP-1 (8.97-fold, 5.18-fold, 2.86-fold, vs 56.58-fold, all $P<0.001$). Moreover, 50 μg/mL and 100 μg/mL Mag also substantially reduced the mRNA of TNF-α (12.49-fold, 7.48-fold, vs 34.07-fold, both $P<0.05$) and IL-6 (163.6-fold, 132.8-fold, vs 354.7-fold, both $P<0.01$) (Figure 7B). Finally, different doses of Mag did not significantly inhibit the expression of iNOS.

ELISA analysis of the supernatant revealed that LPS raised the levels of IL-6, IL-1β, and MCP-1 in the PMs (Figure 7C), but the release of IL-6 (73.04±0.75, 67.97±0.60, 48.17±1.44, vs 102.0±3.61pg/mL, all $P<0.01$), and IL-1β (80.70±6.18, 61.43±0.76, 44.80±0.45, vs 94.80±4.49pg/mL, all $P<0.05$) decreased markedly in the PMs pre-treated with different doses of Mag. Compared to the LPS-stimulated group, low dose of Mag (25 μg/mL) had no significant effects on the release of TNF-α (578.4±0.50 vs 568.4±35.81pg/mL, $P > 0.05$), however, 50 μg/mL and 100 μg/mL Mag both markedly reduced the concentration of TNF-α (392.9±6.68, 382.8±25.98, vs 568.4±35.81pg/mL, both $P<0.001$). The levels of MCP-1 were significantly increased upon treatment with Mag (25μg/mL) compared with LPS-stimulated group (23.58±0.07 vs 20.47

A

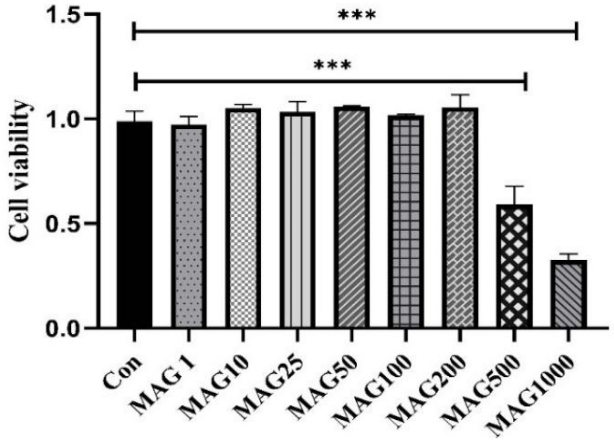

B

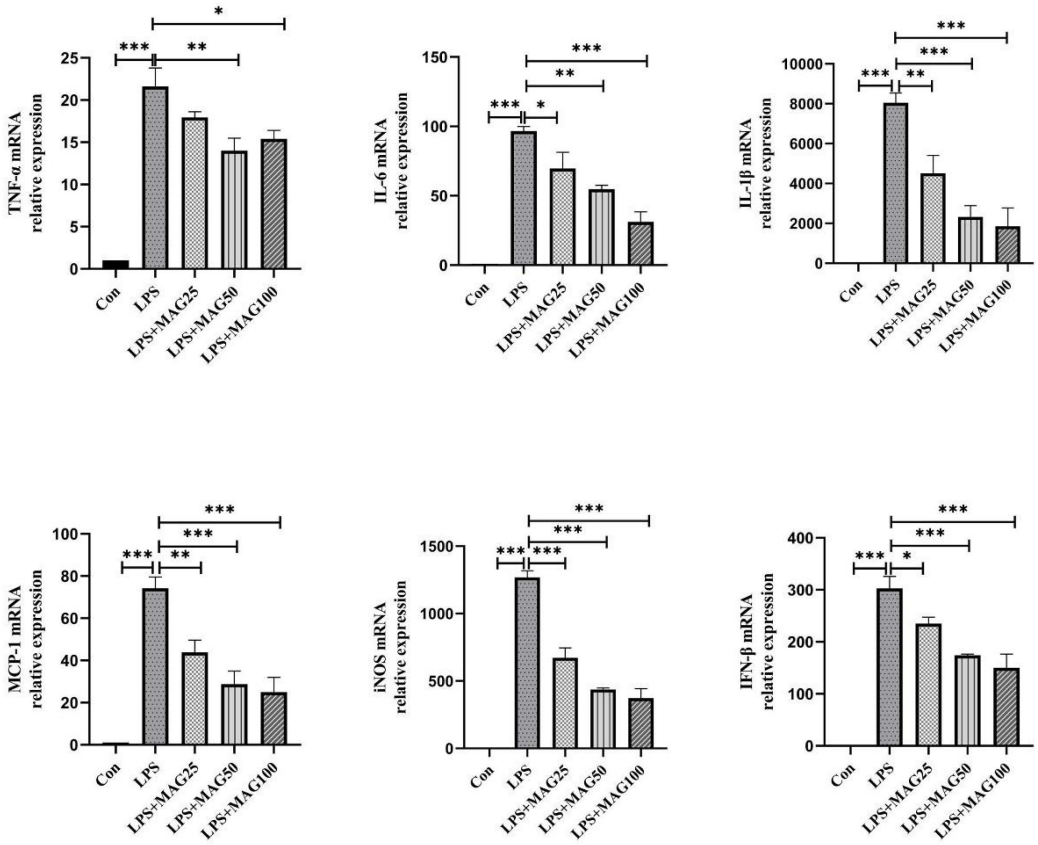

Figure 6 Continued.

C

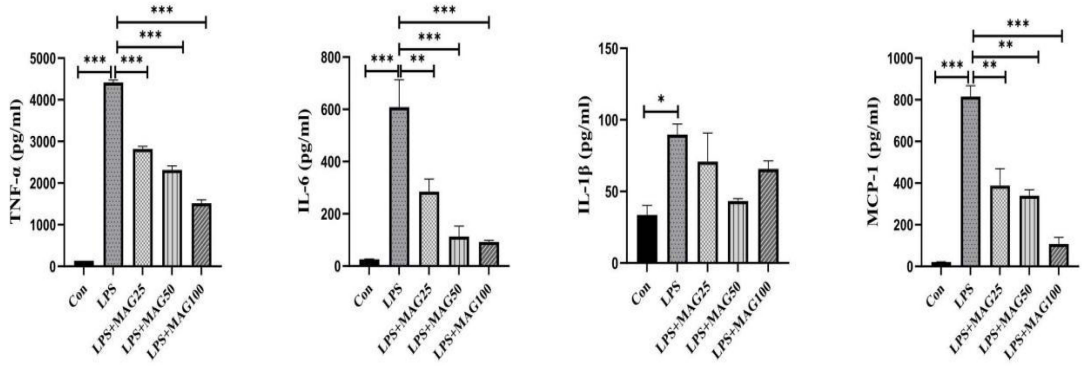

Figure 6 The effects of Mag on the pro-inflammatory cytokines, mediators, and chemokines in LPS-stimulated RAW264.7 cells. (**A**) The cytotoxicity of Mag on RAW264.7 cells was detected by Cell Counting Kit-8 assay. (**B**) The mRNA expression of TNF-α, IL-6, IL-1β, MCP-1, iNOS, and IFN-β in RAW264.7 cells were examined by qRT-PCR. (**C**) ELISA was used to detect the concentrations of TNF-α, IL-6, IL-1β, and MCP-1 in the supernatant of the RAW264.7 cells in each group. Data in (**A**–**C**) are representative of at least three repetitions. **P*<0.05, ***P*<0.01, ****P*<0.001 (one-way ANOVA with Tukey's post hoc test or Kruskal–Wallis test).
Abbreviations: Mag, magnoflorine; ELISA, enzyme linked immunosorbent assay; TNF-α, tumor necrosis factor; IL-6, interleukin-6; IL-1β, interleukin-1β; MCP-1, monocyte chemoattractant protein-1; iNOS, inducible nitric oxide synthase; IFN-β, interferon-beta; qRT-PCR, Quantitative Real-Time PCR; LPS, lipopolysaccharide.

±0.19pg/mL, $P < 0.05$), but the levels of the MCP-1 (16.73±0.34, 14.16±0.07 vs 20.47±0.19pg/mL, both $P < 0.001$) were significantly decreased after treatment with middle and high concentrations of Mag (50 μg/mL and 100 μg/mL), respectively.

Mag Blocks the NF-κB and MAPK Pathways' Activation in LPS-Induced RAW264.7 Cells and the Ankle Joints of CIA Mice

The NF-κB and MAPK signaling pathways are essential for the secretion of the TLR-mediated cytokines. To scrutinize whether Mag regulates the activation of NF-κB and MAPK pathways in the ankle joints of CIA mice, the proteins of p-p65, p-IκBα, p-ERK1/2, and p-p38 MAPK were examined by immunohistochemistry. As shown in Figure 8A and B, increased AOD of p-p65 (0.61±0.01 vs 0.17±0.04, $P < 0.001$), p-IκBα (0.49±0.01 vs 0.33±0.02, $P < 0.01$), p-ERK1/2 (0.57±0.00 vs 0.20±0.01, $P < 0.001$), and p-p38 MAPK (0.58±0.02 vs 0.25±0.03, $P < 0.001$) illustrated activation of the NF-κB and MAPK pathways in the ankle joints of the CIA mice. However, treatment with Mag or MTX showed a remarkable decrease of p-p65 (0.49±0.03, 0.34±0.02, 0.24±0.03, 0.31±0.01, vs 0.61±0.01, all $P < 0.01$), p-ERK1/2 (0.40±0.01, 0.34±0.00, 0.32±0.01, 0.44±0.01, vs 0.57±0.00, all $P < 0.001$) and p-p38 MAPK (0.38±0.02, 0.30±0.01, 0.26 ±0.01, vs 0.58±0.02, all $P < 0.001$) in the ankle joints. Moreover, high doses of Mag obviously reduced p-IκBα (0.35 ±0.01 vs 0.49±0.01, $P<0.05$), whereas low and middle doses of Mag had no significant effects on p-IκBα.

In addition, Western blotting results illustrated that LPS activated the phosphorylation of p65 (0.24±0.05 vs 0.03 ±0.00, $P < 0.001$), IκBα (1.43±0.23 vs 0.14±0.01, $P < 0.01$, ERK1/2 (1.42±0.13 vs 0.15±0.03, $P < 0.001$), p38 MAPK (1.82±0.15 vs 0.16±0.04, $P < 0.001$), and JNK (2.16±0.55 vs 0.19±0.05, $P < 0.001$) in the RAW264.7 cells. As demonstrated in Figure 8C and D, Mag effectively suppressed the expression of phosphorylated ERK1/2 (0.93±0.41, 0.70±0.15, 0.33±0.15 vs 1.42±0.13, all $P < 0.05$), p38 MAPK (1.10±0.25, 1.03±0.02, 0.51±0.21 vs 1.82±0.15, all $P < 0.05$), and JNK (1.10±0.25, 0.96±0.18, 0.78±0.06 vs 2.16±0.55, all $P < 0.05$) in LPS-treated RAW264.7 cells. Moreover, the phosphorylation of p65 (0.16±0.01 vs 0.24±0.05, $P < 0.05$) and IκBα (0.66±0.15 vs 1.43±0.23, $P < 0.05$) was significantly inhibited by 100 μg/mL Mag.

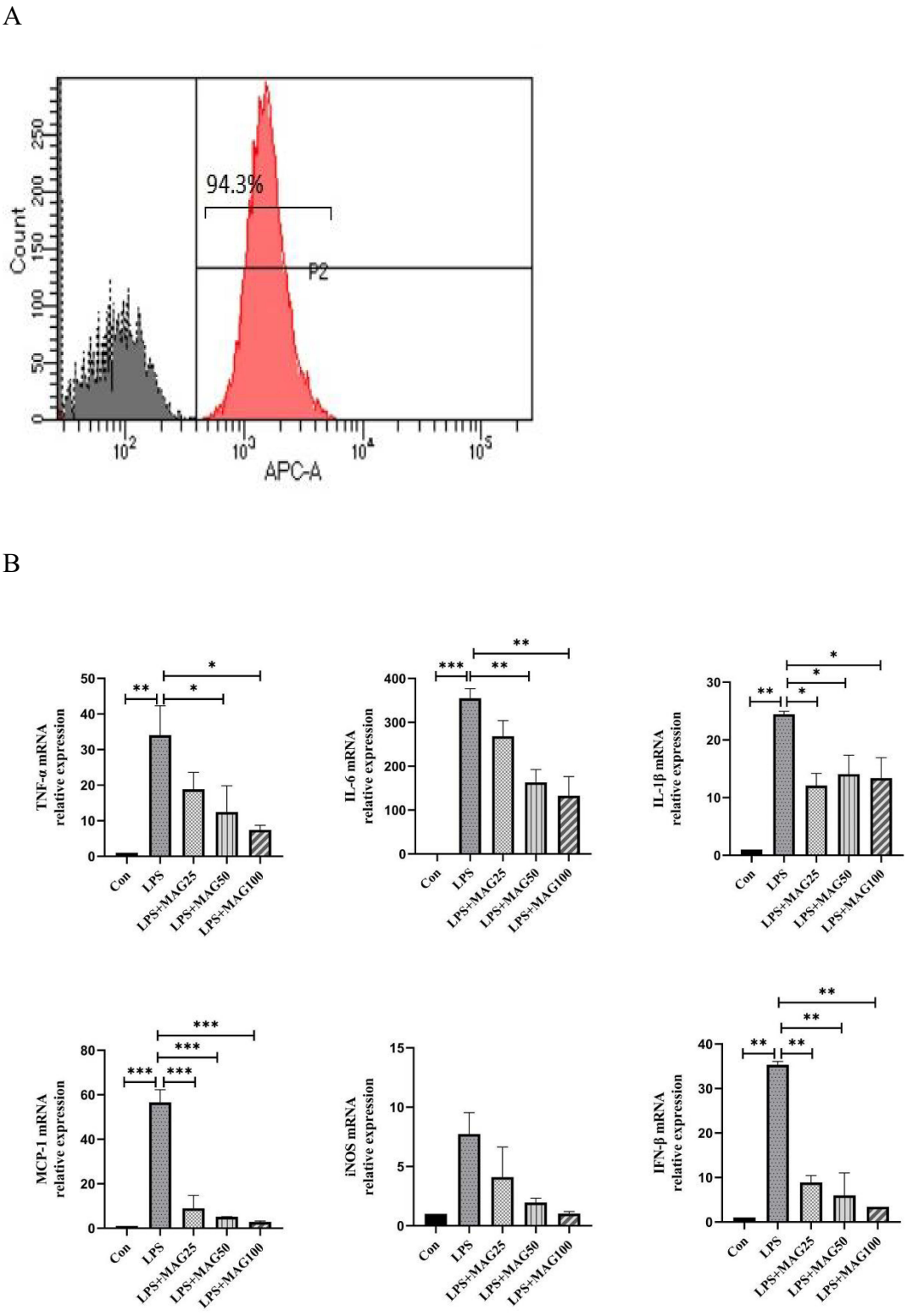

Figure 7 Continued.

C

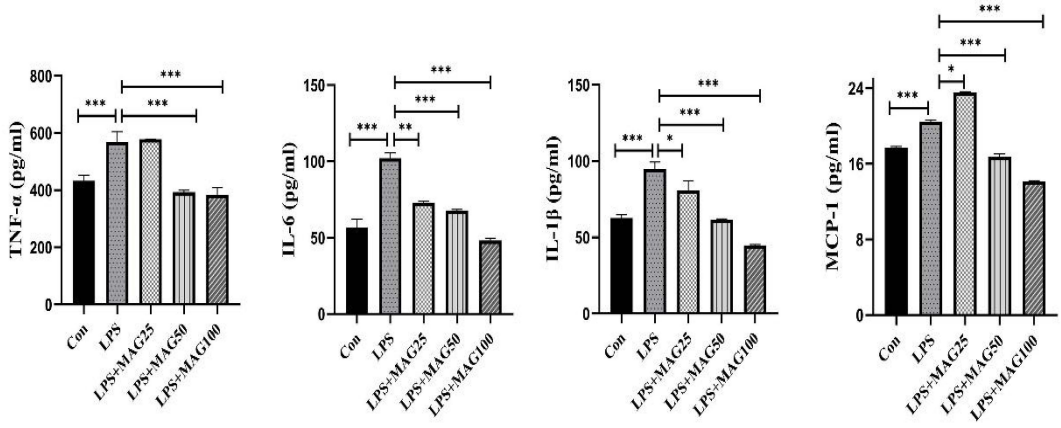

Figure 7 The effects of Mag on the pro-inflammatory cytokines, mediators, and chemokines of LPS-stimulated peritoneal macrophages. (**A**) The proportion of macrophages in the peritoneal cells from mice were detected by flow cytometry. Representative overlay histograms. Gray-filled histograms indicate isotype control. (**B**) The mRNA expression of TNF-α, IL-6, IL-1β, MCP-1, iNOS, and IFN-β mRNA in LPS-induced peritoneal macrophages were determined by qRT-PCR. (**C**) ELISA was used to detect the concentrations of TNF-α, IL-6, IL-1β, and MCP-1 in the peritoneal macrophages. Data in (**A**–**C**) are representative of at least three repetitions. **P*<0.05, ***P*<0.01, ****P*<0.001 (one-way ANOVA with Tukey's post hoc test or Kruskal–Wallis test).

Abbreviations: Mag, magnoflorine; ELISA, enzyme linked immunosorbent assay; TNF-α, tumor necrosis factor; IL-6, interleukin-6; IL-1β, interleukin-1β; MCP-1, monocyte chemoattractant protein-1; iNOS, inducible nitric oxide synthase; IFN-β, interferon-beta; qRT-PCR, Quantitative Real-Time PCR; LPS, lipopolysaccharide.

Discussion

In this study, we demonstrated that the therapeutic effect of Mag on CIA mice and found that Mag exerted its anti-inflammatory via inhibiting the activation of NF-κB and MAPK signaling pathway. Our findings provide a novel evidence to elucidate the therapeutic effects and underlying mechanisms of Mag for treating RA.

The biological agents for RA treatment include anti-TNF, anti-IL-6, and Janus kinase (JAK) inhibitors. Unfortunately, the high cost of these biological agents and the fact that a few of the patients showed an inadequate response, loss of response, or intolerance to them limits their wide application in RA treatment.[37] However, there are some studies showing that TCM has been employed to treat RA in China because of its excellent curative effects and few adverse reactions.[38–40] Caulis Sinomenii has been widely applied to the treatment of RA and osteoporosis.[4] Its major contents are active alkaloids, such as sinomenine and magnoflorine. It has been demonstrated that sinomenine exerted potential anti-rheumatoid arthritis effects through inhibiting the angiogenesis, synovial hyperplasia, bone destruction, and secretion of cytokines.[7,38] Nevertheless, the effects and molecular mechanism of Mag in the treatment of RA was still unclear. We investigated the efficacy and determined the potential mechanism of Mag in RA treatment. The effects of a single Chinese medicine or compound that mainly contains Mag on RA is poised to continue to be the focus of research in the future.

Network pharmacology is an emerging approach that integrates system biology, network analysis, computer, and pharmacology to estimate drug targets and develop multi-target agents of TCM.[41] There is a growing number of research papers that have used the network pharmacology to elucidate the mechanism of TCM in treatment of RA.[42–45] Therefore, in this work, we applied network pharmacology as well as molecular docking to predict and shed light on the potential molecular mechanisms of action of Mag on RA. The results showed that the intersection of Mag targets and RA targets contained 6 genes: *ACHE, PXR, PTGS2, PTGS1, RXRA* and *CA2*. Among them, the PTGS2 and PTGS1 are abundantly produced in inflammatory areas and are closely related to inflammation.[46] More recently, researchers have reported that the expression of pro-inflammatory factors (PTGS2 and PTGS1) were elevated in the synovium of RA patients.[47] Since NSAIDs, cyclooxygenase-2 (COX-2) selective inhibitors, have been extensively used in the treatment of RA, PTGS2, also called COX-2,[48] has been recognized as a therapeutic target of RA.[49] Interestingly, multiple recent findings have also shown

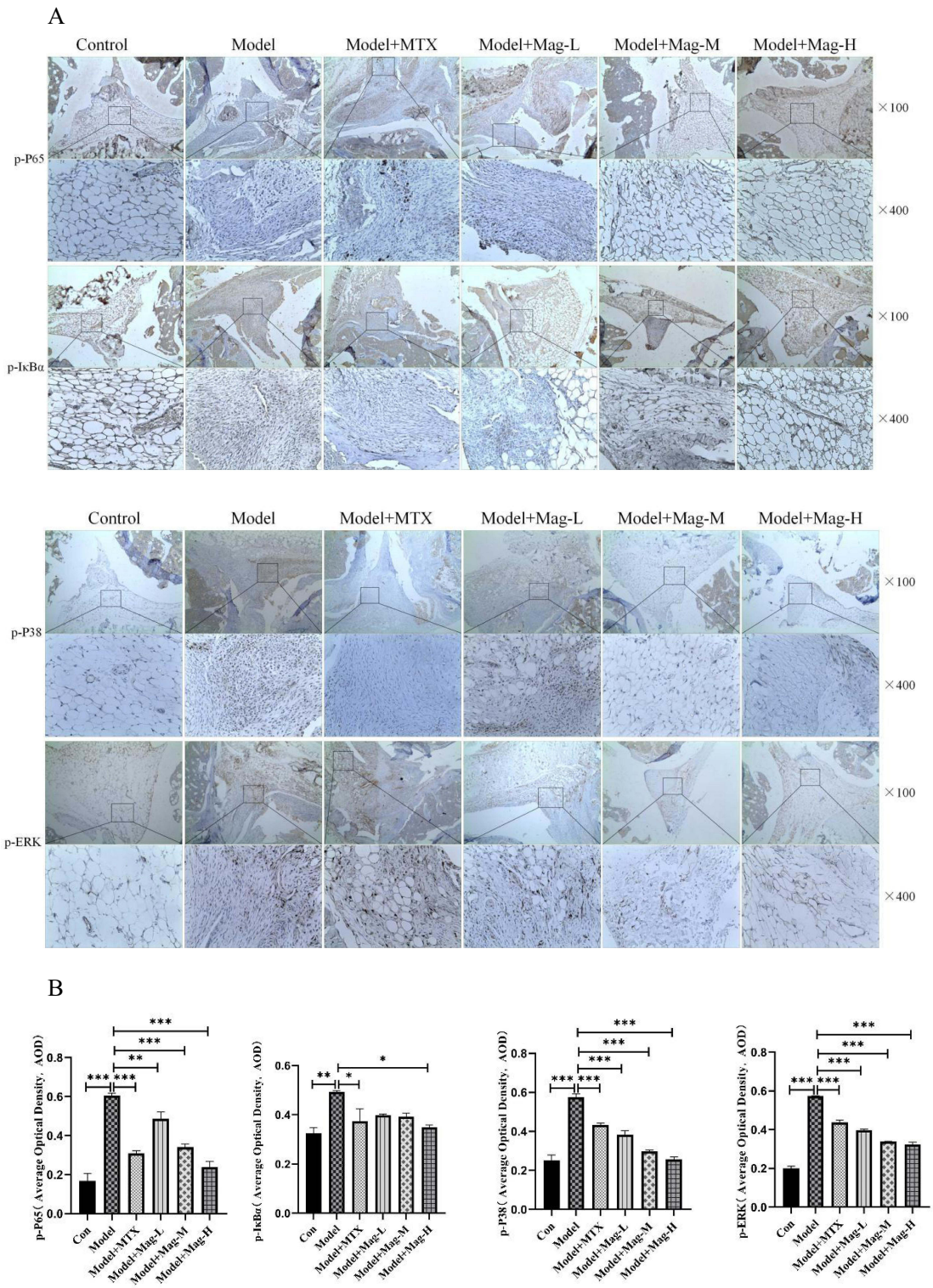

Figure 8 Continued.

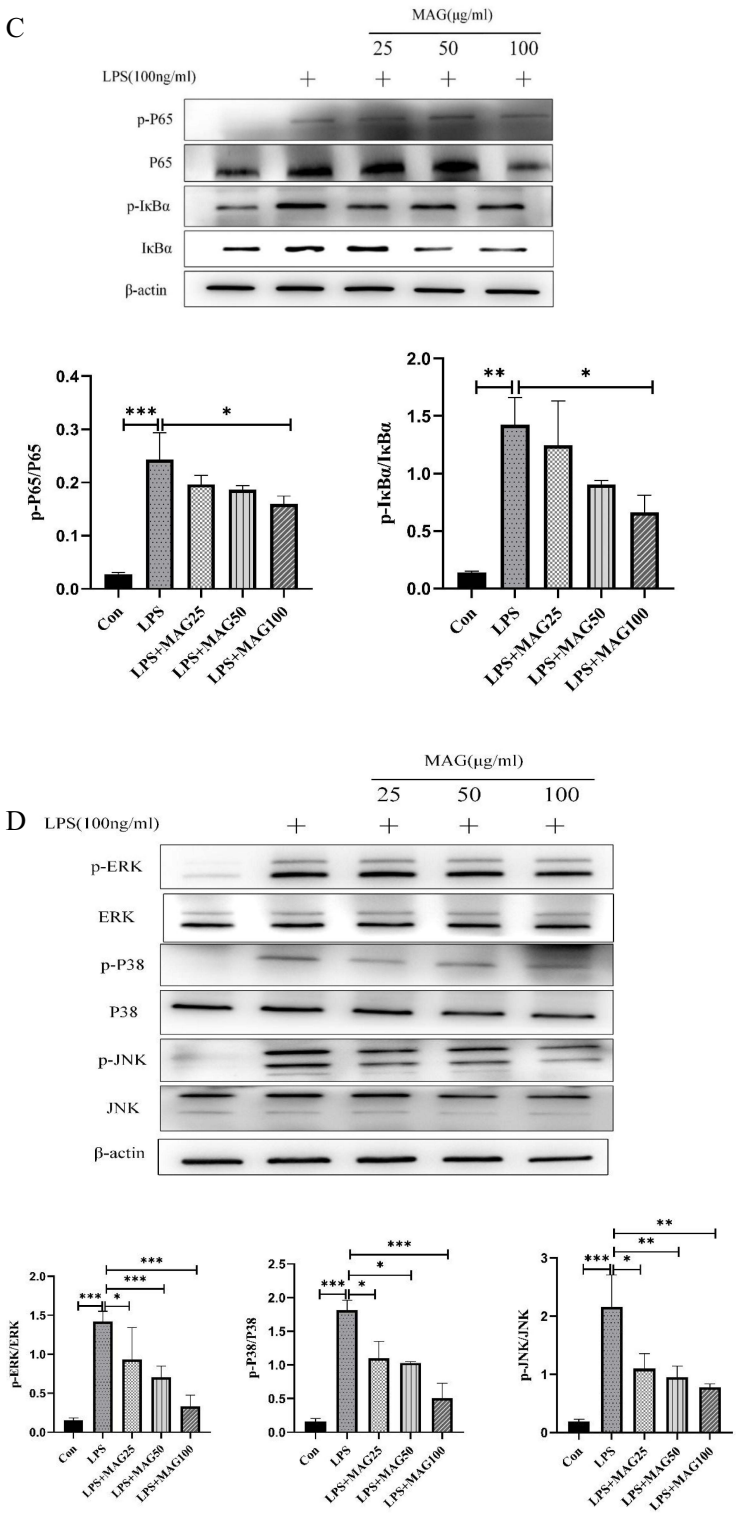

Figure 8 The effects of Mag on the activation of the NF-κB/MAPK signaling pathways in the synovial tissues of CIA mice and LPS-induced RAW264.7 cells. (**A**) Representative photomicrographs of p-p65, p-IκBα, p-ERK1/2, and p-p38 MAPK in the synovial tissues of mice stained by immunohistochemistry (magnification, ×100, ×400). (**B**) The average optical density of p-p65, p-IκBα, p-ERK1/2, and p-p38 MAPK in the synovial tissues of the mice in each group were quantitatively analyzed by Image J software (n = 15). (**C**) The protein levels of the NF-κB signaling pathway in LPS-induced RAW264.7 cells were evaluated by WB. The blots were quantitatively analyzed using the ratio of mean gray. (**D**) The protein level of MAPK signaling pathway in LPS-induced RAW264.7 cells were evaluated by WB as well using the ratio of mean gray. Each experiment was repeated at least three times. *P<0.05, **P<0.01, ***P<0.001 (one-way ANOVA with Tukey's post hoc test).

Abbreviations: Mag, magnoflorine; LPS, lipopolysaccharide; CIA, collagen induced arthritis; WB, Western blotting; NF-κB, nuclear factor-kappa B; MAPK, mitogenactivated protein kinase; p-p65, phospho-p65; p-IκBα, phospho-inhibitory subunit of NF kappa b alpha; p-ERK1/2, phospho-extracellular regulating kinase (ERK)1/2; p-p38 MAPK, phospho-p38 MAPK.

that inhibitors of ACHE or CA2 and PXR agonists attenuate the inflammation and immune dysfunction in RA.[50–53] Collectively, these molecules may be the potential targets of Mag in the treatment of RA. Validation of these potential targets will be conducted by wet lab experiments in our future study.

Molecular docking was performed in this study to predict whether Mag binds to inflammatory cytokines (TNF-α, IL-6, and IL-1β). Scholars have already reported Mag dose-dependently reduced the expression of pro-inflammatory cytokines (TNF-α, IL-1β, and IL-6) in acute lung injury mice.[54] Moreover, a previous study reported that Mag showed an anti-inflammatory effect, and protected LPS-induced macrophage cells by inhibiting the release of inflammation cytokines such as TNF-α, IL-1β, and IL-6.[9] Therefore, based on its observed pharmacological properties, we speculate that Mag exerts anti-inflammatory effects, perhaps by decreasing the levels of pro-inflammatory cytokines. In our future study, bio-layer interferometry (BLI) assay will be performed to determine the binding affinities of Mag with TNF-α, IL-6, IL-1β, and MCP-1.

At present, there is still controversy surrounding the effects of Mag on macrophage and immune response. Recent study has reported that Mag reduced the levels of inflammatory cytokines in IL-1β-treated MH7A cells via the PI3K/Akt/NF-κB signaling axis and attenuated inflammatory responses in adjuvant-induced arthritis rats.[55] Mag can directly attenuate articular cartilage degeneration through activating the chondrogenic signaling pathway to promote proliferation, chondrogenesis and migration of chondroprogenitor cell in a traumatic osteoarthritis model.[56] Notably, Mag has also been found to enhance LPS-activated pro-inflammatory responses via activation of the NF-κB, MAPKs, and PI3K/Akt signaling pathways in LPS-induced U937 human macrophages.[12] In addition, the recent research has shown that Mag induced the chemotaxis, phagocytic activity, and significantly enhances the production of inflammatory mediators and pro-inflammatory cytokines in RAW264.7 macrophages.[57] These authors further reported that Mag stimulated various humoral and cellular immune factors in innate and adaptive immune responses in Balb/c mice.[58] In contrast, Mag has been found to ablate inflammatory response in LPS-induced RAW264.7 cells, possibly through the inhibition of the Toll-like receptor 4-mediated NF-κB and MAPK pathways.[54] Similarly, Mag attenuates LPS-induced THP-1 cells by down-regulating the HMGB1/MyD88/NF-κB pathway and the NACHT-, LRR-, and PYD-domains-containing protein 3 (NLRP3) inflammasome.[11] In this work, we found that Mag exhibited both in vivo and in vitro anti-inflammatory activity by suppressing the production of pro-inflammatory cytokines in CIA mice and LPS-induced macrophages.

It has been demonstrated that macrophages secreted a variety of cytokines and chemokines that enhanced inflammation and contributed to the destruction of cartilage and bone.[13,59] Depletion of macrophages also improves symptoms in mouse models of RA.[60] Therefore, targeting macrophages has emerged as a potential treatment strategy for RA. The F4/80$^+$ macrophages are higher in the ankle joints of CIA mice,[61] and CD68$^+$ macrophages are a type of pro-inflammatory macrophages, that is distinctly higher in the synovial tissues of adjuvant-induced arthritis rats.[36] In addition, the number of synovial CD68$^+$ macrophages correlates with disease activity scores for RA.[62,63] Moreover, it has been proposed that CD68, a phenotypic marker of synovial macrophages, may be an optimal marker to evaluate the therapeutic response in RA clinical trials. Celastrol, a bioactive compound derived from Tripterygium wilfordii and Celastrus orbiculatus, ameliorated local joint inflammation and bone damage in AIA Rats reduces CD68$^+$ macrophages in the arthritic synovial tissue.[64] In our study, different doses of Mag markedly decreased the expression of both F4/80 and CD68 in ankle synovial tissue from CIA mice. Therefore, we speculated that Mag inhibited the number of macrophages in synovial tissue of CIA mice. Overall, our research also elaborated that Mag protected against RA by regulating the immune response of macrophages and reducing the infiltration of CD68$^+$ macrophages into the synovial tissues.

The NF-κB signaling pathway has been identified as one of the main inflammatory pathways responsible for the secretion of inflammatory cytokines, and it can regulate the immune response in RA.[65] Research has indicated that sinomenine reduced the expression of p65 and p-p65 in RA FLSs by alleviating the joints damage of adjuvant arthritis rats.[66] A recent study has also reported that C-X-C chemokine receptor type 3 (CXCR3) antagonist AMG487 exerted the anti-arthritic effects in CIA mice by suppressing inflammatory response via the NF-κB signaling pathway.[67] Furthermore, Ahmad et al have demonstrated that signal transducer and activator of transcription 3 (STAT-3) inhibitor attenuates the development and progression of inflammation in CIA mice by inhibiting cellular signaling pathways, such as NF-κB p65, JAK1, and STAT-3.[68] Moreover, it was reported that Mag effectively prevented peri-implant osteolysis through the inhibition of activation of MAPK and NF-kB signaling pathways.[10] In this study, we found that Mag significantly

decreased the expression of p-p65 in synovial tissues from CIA mice. The expression of the MAPK signaling pathway in the synovial tissues was also observed. The MAPK pathway is responsible for regulating the production of pro-inflammatory cytokines, leading to joint inflammation and destruction.[69] Our results indicated that the expression of p-ERK1/2 and p-p38 markedly decreased in the synovial tissues of the Mag-treated CIA mice. These results show that the anti-inflammatory effects of Mag were mediated by the NF-κB/MAPK pathways.

The NF-κB/MAPK signaling pathways are triggered by LPS and participate in the release of inflammatory factors in macrophages.[70] In this study, we observed that Mag significantly reduced the phosphorylation levels of p65, IκBα, ERK, p38 MAPK, and JNK induced by LPS. These results suggested that Mag inhibited the LPS-primed macrophages inflammatory responses through the NF-κB/MAPK signaling pathways. One previous study found that chelidonine suppressed the inflammatory factors such as iNOS by inhibiting the phosphorylation of p65 and IκBα in the NF-κB pathway.[71] Another recent study revealed that the inhibition of phosphorylation of ERK, p38 and JNK in the MAPK pathway reduced LPS-induced TNF-α and IL-6 production in macrophages.[72] These findings show that the inflammatory factors in LPS-stimulated macrophages may be inhibited by the inactivation of the NF-κB/MAPK signaling pathways.

In this study, primary PMs and RAW264.7 cells line were used to induce inflammatory models by LPS. Several reports have already indicated LPS stimulated the expression and secretion of pro-inflammatory cytokines TNF-α, IL-6, and IL-1β in RAW264.7 cells.[73,74] Our results revealed that the expression of TNF-α, IL-6, IL-1β, MCP-1, iNOS, and IFN-β increased in LPS-induced macrophages. Furthermore, our findings also illustrated that the expression of pro-inflammatory cytokines were enhanced in the synovial tissues, PMs, and serum of CIA mice. Growing evidence also shows that there are changes in inflammatory cytokines in RA. Wang et al have reported elevated levels of TNF-α and IL-6 in the serum and synovial tissues of RA patients and CIA mice,[75] and others have also reported that hesperidin reduced the pro-inflammatory cytokines TNF-α, IL-6, and IL-17A in the serum of CIA mice.[76] Ansari et al have shown that chemokine receptor 5 antagonism shows potent anti-arthritic effects on CIA mice by reducing joint inflammation.[77] Pro-inflammatory markers, including iNOS, TNF-α, and, IL-6 are typically elevated in CIA mice.[78] In this study, we found that the expression of iNOS, TNF-α, and IL-6 were up-regulated in the synovium and PMs of CIA mice. In addition, Mag down-regulated the expression of inflammatory cytokines in the macrophages, serum, and synovial tissues of CIA mice. These results indicated that Mag exhibited anti-inflammatory effects in vitro and in vivo.

This work provides a novel mechanism of Mag in the treatment of RA. However, there are some limitations to this study. First, the mechanism involved in the anti-arthritis effect of Mag has not been fully elucidated. A multitude of other types of cells contribute to the complex RA pathogenesis such as synovial fibroblasts, B cells, T cells, and neutrophils.[79] Our study mainly focused on the role of Mag in regulating macrophages. Accordingly, investigations are needed to clarify the effects and underlying mechanism of Mag's effects on other types of cells in RA. Second, further clinical research is needed to confirm the anti-arthritis effects of Mag in RA patients in the future.

Conclusion

Overall, our present research revealed Mag attenuated the inflammatory response in LPS-induced RAW264.7 cells and PMs in vitro and CIA mice in vivo. MAG may thus alleviate the severity of CIA in mice by repressing the NF-κB/MAPK signaling pathways.

Acknowledgments

This work was supported by National Natural Science Foundation of China (Grant No. 11574156); and Foundation of State Key Laboratory of Ultrasound in Medicine and Engineering (Grant No. 2022KFKT021); and 333 Project of Jiangsu Province, China (Grant No. BRA2018088).

Disclosure

The authors have declared that no competing interest exists in this work.

References

1. Zhou Y, Wang X, An Y, et al. Disability and health-related quality of life in Chinese patients with rheumatoid arthritis: a cross-sectional study. *Int J Rheum Dis*. 2018;21(9):1709–1715. doi:10.1111/1756-185X.13345
2. Arleevskaya MI, Larionova RV, Brooks WH, Bettacchioli E, Renaudineau Y. Toll-like receptors, infections, and rheumatoid arthritis. *Clin Rev Allergy Immunol*. 2020;58(2):172–181. doi:10.1007/s12016-019-08742-z
3. Zhou WZ, Miao LG, Yuan H. Identification of significant ego networks and pathways in rheumatoid arthritis. *J Cancer Res Ther*. 2018;14 (Supplement):S1024–S1028. doi:10.4103/0973-1482.189250
4. Liu WJ, Jiang ZM, Chen Y, et al. Network pharmacology approach to elucidate possible action mechanisms of Sinomenii Caulis for treating osteoporosis. *J Ethnopharmacol*. 2020;257:112871. doi:10.1016/j.jep.2020.112871
5. Sakumoto H, Yokota Y, Ishibashi G, et al. Sinomenine and magnoflorine, major constituents of Sinomeni caulis et rhizoma, show potent protective effects against membrane damage induced by lysophosphatidylcholine in rat erythrocytes. *J Nat Med*. 2015;69(3):441–448. doi:10.1007/s11418-015-0907-7
6. de Seabra Rodrigues Dias IR, Lo HH, Zhang K, et al. Potential therapeutic compounds from traditional Chinese medicine targeting endoplasmic reticulum stress to alleviate rheumatoid arthritis. *Pharmacol Res*. 2021;170:105696. doi:10.1016/j.phrs.2021.105696
7. Liu W, Zhang Y, Zhu W, et al. Sinomenine inhibits the progression of rheumatoid arthritis by regulating the secretion of inflammatory cytokines and monocyte/macrophage subsets. *Front Immunol*. 2018;9:2228. doi:10.3389/fimmu.2018.02228
8. Yi L, Ke J, Liu J, et al. Sinomenine increases adenosine A2A receptor and inhibits NF-kappaB to inhibit arthritis in adjuvant-induced-arthritis rats and fibroblast-like synoviocytes through alpha7nAChR. *J Leukoc Biol*. 2021;110(6):1113–1120. doi:10.1002/JLB.3MA0121-024RRRR
9. Xu T, Kuang T, Du H, et al. Magnoflorine: a review of its pharmacology, pharmacokinetics and toxicity. *Pharmacol Res*. 2020;152:104632. doi:10.1016/j.phrs.2020.104632
10. Sun Z, Zeng J, Wang W, et al. Magnoflorine suppresses MAPK and NF-kappaB signaling to prevent inflammatory osteolysis induced by titanium particles in vivo and osteoclastogenesis via RANKL in vitro. *Front Pharmacol*. 2020;11:389. doi:10.3389/fphar.2020.00389
11. Zhao F, Guo Z, Hou F, Fan W, Wu B, Qian Z. Magnoflorine alleviates "M1" polarized macrophage-induced intervertebral disc degeneration through repressing the HMGB1/Myd88/NF-kappaB pathway and NLRP3 inflammasome. *Front Pharmacol*. 2021;12:701087. doi:10.3389/fphar.2021.701087
12. Haque MA, Jantan I, Harikrishnan H, Abdul Wahab SM. Magnoflorine enhances LPS-activated pro-inflammatory responses via MyD88-dependent pathways in U937 macrophages. *Planta Med*. 2018;84(17):1255–1264. doi:10.1055/a-0637-9936
13. Udalova IA, Mantovani A, Feldmann M. Macrophage heterogeneity in the context of rheumatoid arthritis. *Nat Rev Rheumatol*. 2016;12 (8):472–485. doi:10.1038/nrrheum.2016.91
14. Edilova MI, Akram A, Abdul-Sater AA. Innate immunity drives pathogenesis of rheumatoid arthritis. *Biomed J*. 2021;44(2):172–182. doi:10.1016/j.bj.2020.06.010
15. Tardito S, Martinelli G, Soldano S, et al. Macrophage M1/M2 polarization and rheumatoid arthritis: a systematic review. *Autoimmun Rev*. 2019;18 (11):102397. doi:10.1016/j.autrev.2019.102397
16. Ross EA, Devitt A, Johnson JR. Macrophages: the good, the bad, and the gluttony. *Front Immunol*. 2021;12:708186. doi:10.3389/fimmu.2021.708186
17. Brand DD, Latham KA, Rosloniec EF. Collagen-induced arthritis. *Nat Protoc*. 2007;2(5):1269–1275. doi:10.1038/nprot.2007.173
18. Liu Y, Zhang L, Wu Y, et al. Therapeutic effects of TACI-Ig on collagen-induced arthritis by regulating T and B lymphocytes function in DBA/1 mice. *Eur J Pharmacol*. 2011;654(3):304–314. doi:10.1016/j.ejphar.2011.01.002
19. Das NM, Hatsell S, Nannuru K, et al. In vivo quantitative microcomputed tomographic analysis of vasculature and organs in a normal and diseased mouse model. *PLoS One*. 2016;11(2):e0150085. doi:10.1371/journal.pone.0150085
20. El-Waseef D. A highlight on CD4(+) T-cells in the spleen in a rat model of rheumatoid arthritis and possible therapeutic effect of omega-3. Histological and Immunofluorescence study. *Int Immunopharmacol*. 2020;81:106283. doi:10.1016/j.intimp.2020.106283
21. Ru J, Li P, Wang J, et al. TCMSP: a database of systems pharmacology for drug discovery from herbal medicines. *J Cheminform*. 2014;6:13. doi:10.1186/1758-2946-6-13
22. Liu Z, Guo F, Wang Y, et al. BATMAN-TCM: a bioinformatics analysis tool for molecular mechANism of traditional Chinese medicine. *Sci Rep*. 2016;6:21146. doi:10.1038/srep21146
23. Wang Y, Bryant SH, Cheng T, et al. PubChem BioAssay: 2017 update. *Nucleic Acids Res*. 2017;45(D1):D955–D963. doi:10.1093/nar/gkw1118
24. Szklarczyk D, Santos A, von Mering C, Jensen LJ, Bork P, Kuhn M. STITCH 5: augmenting protein-chemical interaction networks with tissue and affinity data. *Nucleic Acids Res*. 2016;44(D1):D380–384. doi:10.1093/nar/gkv1277
25. Hamosh A, Scott AF, Amberger JS, Bocchini CA, McKusick VA. Online Mendelian Inheritance in Man (OMIM), a knowledgebase of human genes and genetic disorders. *Nucleic Acids Res*. 2005;33(Database issue):D514–517. doi:10.1093/nar/gki033
26. Rebhan M, Chalifa-Caspi V, Prilusky J, Lancet D. GeneCards: integrating information about genes, proteins and diseases. *Trends Genet*. 1997;13 (4):163. doi:10.1016/S0168-9525(97)01103-7
27. Wishart DS, Knox C, Guo AC, et al. DrugBank: a knowledgebase for drugs, drug actions and drug targets. *Nucleic Acids Res*. 2008;36(Database issue):D901–906. doi:10.1093/nar/gkm958
28. Newman DJ. Modern traditional Chinese medicine: identifying, defining and usage of TCM components. *Adv Pharmacol*. 2020;87:113–158.
29. Behzadi P, Gajdacs M. Worldwide Protein Data Bank (wwPDB): a virtual treasure for research in biotechnology. *Eur J Microbiol Immunol (Bp)*. 2022;11(4):77–86. doi:10.1556/1886.2021.00020
30. Seeliger D, de Groot BL. Ligand docking and binding site analysis with PyMOL and Autodock/Vina. *J Comput Aided Mol Des*. 2010;24 (5):417–422. doi:10.1007/s10822-010-9352-6
31. Dos Anjos Cassado A. F4/80 as a major macrophage marker: the case of the peritoneum and spleen. *Results Probl Cell Differ*. 2017;62:161–179.
32. Wang Q, Ye C, Sun S, et al. Curcumin attenuates collagen-induced rat arthritis via anti-inflammatory and apoptotic effects. *Int Immunopharmacol*. 2019;72:292–300. doi:10.1016/j.intimp.2019.04.027
33. Schmittgen TD, Livak KJ. Analyzing real-time PCR data by the comparative C(T) method. *Nat Protoc*. 2008;3(6):1101–1108. doi:10.1038/nprot.2008.73

34. Wang Q, Zhou X, Zhao Y, et al. Polyphyllin I ameliorates collagen-induced arthritis by suppressing the inflammation response in macrophages through the NF-kappaB pathway. *Front Immunol*. 2018;9:2091. doi:10.3389/fimmu.2018.02091
35. Simpson RJ. Quantifying protein by bicinchoninic Acid. *CSH Protoc*. 2008;2008:pdb prot4722. doi:10.1101/pdb.prot4722
36. Abdel Jaleel GA, Azab SS, El-Bakly WM, Hassan A. Methyl palmitate attenuates adjuvant induced arthritis in rats by decrease of CD68 synovial macrophages. *Biomed Pharmacother*. 2021;137:111347. doi:10.1016/j.biopha.2021.111347
37. Rubbert-Roth A, Szabo MZ, Kedves M, Nagy G, Atzeni F, Sarzi-Puttini P. Failure of anti-TNF treatment in patients with rheumatoid arthritis: the pros and cons of the early use of alternative biological agents. *Autoimmun Rev*. 2019;18(12):102398. doi:10.1016/j.autrev.2019.102398
38. Guo X, Ji J, Feng Z, Hou X, Luo Y, Mei Z. A network pharmacology approach to explore the potential targets underlying the effect of sinomenine on rheumatoid arthritis. *Int Immunopharmacol*. 2020;80:106201. doi:10.1016/j.intimp.2020.106201
39. Wang Y, Chen S, Du K, et al. Traditional herbal medicine: therapeutic potential in rheumatoid arthritis. *J Ethnopharmacol*. 2021;279:114368. doi:10.1016/j.jep.2021.114368
40. Akram M, Daniyal M, Sultana S, et al. Traditional and modern management strategies for rheumatoid arthritis. *Clin Chim Acta*. 2021;512:142–155. doi:10.1016/j.cca.2020.11.003
41. Bai LL, Chen H, Zhou P, Yu J. Identification of tumor necrosis factor-alpha (TNF-alpha) inhibitor in rheumatoid arthritis using network pharmacology and molecular docking. *Front Pharmacol*. 2021;12:690118. doi:10.3389/fphar.2021.690118
42. Song X, Zhang Y, Dai E, Wang L, Du H. Prediction of triptolide targets in rheumatoid arthritis using network pharmacology and molecular docking. *Int Immunopharmacol*. 2020;80:106179. doi:10.1016/j.intimp.2019.106179
43. Wu N, Yuan T, Yin Z, et al. Network pharmacology and molecular docking study of the Chinese miao medicine sidaxue in the treatment of rheumatoid arthritis. *Drug Des Devel Ther*. 2022;16:435–466. doi:10.2147/DDDT.S330947
44. Cui X, Liu J, Zhang L, Wang X, Liu X, Jiang H. Network pharmacology approach and molecular docking to explore the potential mechanism of Wu-Wei-Wen-Tong Chubi capsules in rheumatoid arthritis. *Naunyn Schmiedebergs Arch Pharmacol*. 2022;395(9):1061–1073. doi:10.1007/s00210-022-02260-0
45. Xia X, Zeng H, Wang H, et al. Revealing the active constituents and mechanisms of semiliquidambar cathayensis chang roots against rheumatoid arthritis through network pharmacology, molecular docking, and in vivo experiment. *Chem Biodivers*. 2023;20(1):e202200916. doi:10.1002/cbdv.202200916
46. Tsuge K, Inazumi T, Shimamoto A, Sugimoto Y. Molecular mechanisms underlying prostaglandin E2-exacerbated inflammation and immune diseases. *Int Immunol*. 2019;31(9):597–606. doi:10.1093/intimm/dxz021
47. Kusunoki N, Kitahara K, Kojima F, et al. Adiponectin stimulates prostaglandin E(2) production in rheumatoid arthritis synovial fibroblasts. *Arthritis Rheum*. 2010;62(6):1641–1649. doi:10.1002/art.27450
48. Meriwether D, Jones AE, Ashby JW, et al. Macrophage COX2 mediates efferocytosis, resolution reprogramming, and intestinal epithelial repair. *Cell Mol Gastroenterol Hepatol*. 2022;13(4):1095–1120. doi:10.1016/j.jcmgh.2022.01.002
49. Peng A, Lu X, Huang J, et al. Rheumatoid arthritis synovial fibroblasts promote TREM-1 expression in monocytes via COX-2/PGE(2) pathway. *Arthritis Res Ther*. 2019;21(1):169. doi:10.1186/s13075-019-1954-3
50. Gowayed MA, Rothe K, Rossol M, et al. The role of alpha7nAChR in controlling the anti-inflammatory/anti-arthritic action of galantamine. *Biochem Pharmacol*. 2019;170:113665. doi:10.1016/j.bcp.2019.113665
51. Akgul O, Di Cesare Mannelli L, Vullo D, et al. Discovery of novel nonsteroidal anti-inflammatory drugs and carbonic anhydrase inhibitors hybrids (NSAIDs-CAIs) for the management of rheumatoid arthritis. *J Med Chem*. 2018;61(11):4961–4977. doi:10.1021/acs.jmedchem.8b00420
52. Berrino E, Milazzo L, Micheli L, et al. Synthesis and evaluation of carbonic anhydrase inhibitors with carbon monoxide releasing properties for the management of rheumatoid arthritis. *J Med Chem*. 2019;62(15):7233–7249. doi:10.1021/acs.jmedchem.9b00845
53. Mencarelli A, D'Amore C, Renga B, et al. Solomonsterol A, a marine pregnane-X-receptor agonist, attenuates inflammation and immune dysfunction in a mouse model of arthritis. *Mar Drugs*. 2013;12(1):36–53. doi:10.3390/md12010036
54. Guo S, Jiang K, Wu H, et al. Magnoflorine ameliorates lipopolysaccharide-induced acute lung injury via suppressing NF-kappaB and MAPK activation. *Front Pharmacol*. 2018;9:982. doi:10.3389/fphar.2018.00982
55. Shen Y, Fan X, Qu Y, et al. Magnoflorine attenuates inflammatory responses in RA by regulating the PI3K/Akt/NF-kappaB and Keap1-Nrf2/HO-1 signalling pathways in vivo and in vitro. *Phytomedicine*. 2022;104:154339. doi:10.1016/j.phymed.2022.154339
56. Cai Z, Hong M, Xu L, et al. Prevent action of magnoflorine with hyaluronic acid gel from cartilage degeneration in anterior cruciate ligament transection induced osteoarthritis. *Biomed Pharmacother*. 2020;126:109733. doi:10.1016/j.biopha.2019.109733
57. Ahmad W, Jantan I, Kumolosasi E, Haque MA, Bukhari SNA. Immunomodulatory effects of Tinospora crispa extract and its major compounds on the immune functions of RAW 264.7 macrophages. *Int Immunopharmacol*. 2018;60:141–151. doi:10.1016/j.intimp.2018.04.046
58. Ahmad W, Jantan I, Haque MA, Arsyad L. Magnoflorine from Tinospora crispa upregulates innate and adaptive immune responses in Balb/c mice. *Int Immunopharmacol*. 2022;111:109081. doi:10.1016/j.intimp.2022.109081
59. Weyand CM, Goronzy JJ. The immunology of rheumatoid arthritis. *Nat Immunol*. 2021;22(1):10–18. doi:10.1038/s41590-020-00816-x
60. Hu Y, Wang B, Shen J, et al. Depletion of activated macrophages with a folate receptor-beta-specific antibody improves symptoms in mouse models of rheumatoid arthritis. *Arthritis Res Ther*. 2019;21(1):143. doi:10.1186/s13075-019-1912-0
61. Ye L, Wen Z, Li Y, et al. Interleukin-10 attenuation of collagen-induced arthritis is associated with suppression of interleukin-17 and retinoid-related orphan receptor gammat production in macrophages and repression of classically activated macrophages. *Arthritis Res Ther*. 2014;16(2):R96. doi:10.1186/ar4544
62. Bresnihan B, Pontifex E, Thurlings RM, et al. Synovial tissue sublining CD68 expression is a biomarker of therapeutic response in rheumatoid arthritis clinical trials: consistency across centers. *J Rheumatol*. 2009;36(8):1800–1802. doi:10.3899/jrheum.090348
63. Li J, Hsu HC, Mountz JD. Managing macrophages in rheumatoid arthritis by reform or removal. *Curr Rheumatol Rep*. 2012;14(5):445–454. doi:10.1007/s11926-012-0272-4
64. Cascao R, Vidal B, Lopes IP, et al. Decrease of CD68 synovial macrophages in celastrol treated arthritic rats. *PLoS One*. 2015;10(12):e0142448. doi:10.1371/journal.pone.0142448
65. Ilchovska DD, Barrow DM. An overview of the NF-kB mechanism of pathophysiology in rheumatoid arthritis, investigation of the NF-kB ligand RANKL and related nutritional interventions. *Autoimmun Rev*. 2021;20(2):102741. doi:10.1016/j.autrev.2020.102741

66. Yao RB, Zhao ZM, Zhao LJ, Cai H. Sinomenine inhibits the inflammatory responses of human fibroblast-like synoviocytes via the TLR4/MyD88/NF-kappaB signaling pathway in rheumatoid arthritis. *Pharmazie*. 2017;72(6):355–360. doi:10.1691/ph.2017.6946
67. Bakheet SA, Alrwashied BS, Ansari MA, et al. CXC chemokine receptor 3 antagonist AMG487 shows potent anti-arthritic effects on collagen-induced arthritis by modifying B cell inflammatory profile. *Immunol Lett*. 2020;225:74–81. doi:10.1016/j.imlet.2020.06.014
68. Ahmad SF, Ansari MA, Nadeem A, et al. STA-21, a STAT-3 inhibitor, attenuates the development and progression of inflammation in collagen antibody-induced arthritis. *Immunobiology*. 2017;222(2):206–217. doi:10.1016/j.imbio.2016.10.001
69. Yang G, Chang CC, Yang Y, et al. Resveratrol alleviates rheumatoid arthritis via reducing ROS and inflammation, inhibiting MAPK signaling pathways, and suppressing angiogenesis. *J Agric Food Chem*. 2018;66(49):12953–12960. doi:10.1021/acs.jafc.8b05047
70. Bode JG, Ehlting C, Haussinger D. The macrophage response towards LPS and its control through the p38(MAPK)-STAT3 axis. *Cell Signal*. 2012;24(6):1185–1194. doi:10.1016/j.cellsig.2012.01.018
71. Liao W, He X, Yi Z, Xiang W, Ding Y. Chelidonine suppresses LPS-induced production of inflammatory mediators through the inhibitory of the TLR4/NF-kappaB signaling pathway in RAW264.7 macrophages. *Biomed Pharmacother*. 2018;107:1151–1159. doi:10.1016/j.biopha.2018.08.094
72. Xie C, Li X, Zhu J, Wu J, Geng S, Zhong C. Magnesium isoglycyrrhizinate suppresses LPS-induced inflammation and oxidative stress through inhibiting NF-kappaB and MAPK pathways in RAW264.7 cells. *Bioorg Med Chem*. 2019;27(3):516–524. doi:10.1016/j.bmc.2018.12.033
73. Linghu KG, Ma QS, Zhao GD, et al. Leocarpinolide B attenuates LPS-induced inflammation on RAW264.7 macrophages by mediating NF-kappaB and Nrf2 pathways. *Eur J Pharmacol*. 2020;868:172854. doi:10.1016/j.ejphar.2019.172854
74. Chen JJ, Huang CC, Chang HY, et al. Scutellaria baicalensis ameliorates acute lung injury by suppressing inflammation in vitro and in vivo. *Am J Chin Med*. 2017;45(1):137–157. doi:10.1142/S0192415X17500100
75. Wang Y, Liu R, Zhao P, et al. Blockade of adiponectin receptor 1 signaling inhibits synovial inflammation and alleviates joint damage in collagen-induced arthritis. *Clin Rheumatol*. 2022;41(1):255–264. doi:10.1007/s10067-021-05846-w
76. Babu V, Binwal M, Ranjana R, et al. Hesperidin-rich ethanol extract from waste peels of Citrus limetta mitigates rheumatoid arthritis and related complications. *Phytother Res*. 2021;35(6):3325–3336. doi:10.1002/ptr.7053
77. Ansari MA, Nadeem A, Bakheet SA, et al. Chemokine receptor 5 antagonism causes reduction in joint inflammation in a collagen-induced arthritis mouse model. *Molecules*. 2021;26(7):1839. doi:10.3390/molecules26071839
78. Shen C, Kuang Y, Xu S, et al. Nitidine chloride inhibits fibroblast like synoviocytes-mediated rheumatoid synovial inflammation and joint destruction by targeting KCNH1. *Int Immunopharmacol*. 2021;101(Pt A):108273. doi:10.1016/j.intimp.2021.108273
79. Koga T, Kawakami A, Tsokos GC. Current insights and future prospects for the pathogenesis and treatment for rheumatoid arthritis. *Clin Immunol*. 2021;225:108680. doi:10.1016/j.clim.2021.108680